BRITISH COLUMBIA HYDRO AND POWER AUTHORITY

HAT CREEK PROJECT

Environmental Research and Technology Inc. - Air Quality and Climatic Effects of the Proposed Hat Creek Project Report - Appendix B - Modeling Methodology - April 1978.

ENVIRONMENTAL IMPACT STATEMENT REFERENCE NUMBER: 14c

Document P-5074-F-B
April 1978

Prepared for
British Columbia Hydro and Power Authority

Air quality and climatic effects of the proposed Hat Creek project

Appendix B
Modeling methodology

2030 Alameda Padre Serra
Santa Barbara, California 93103

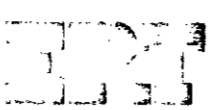

ENVIRONMENTAL RESEARCH & TECHNOLOGY, INC.
CONCORD, MASS. • LOS ANGELES • ATLANTA • SAN JUAN, P.R.
FORT COLLINS, CO. • WASHINGTON, D.C. • HOUSTON • CHICAGO

PRINTED IN U.S.A.

TABLE OF CONTENTS

TABLE OF CONTENTS (Continued)

LIST OF FIGURES

LIST OF TABLES

B1.0 INTRODUCTION

B1.1 MODELING OBJECTIVES

The purpose of this Appendix is to provide British Columbia Hydro & Power Authority (B.C. Hydro) with a detailed discussion of the method used in assessing the effects of contaminants from the proposed Hat Creek Project on local and regional air quality. The Hat Creek Project will consist of a 2000 Mw (nominal) coal-fired electric power plant, an open pit coal mine, and associated facilities. The mine will be located in the Upper Hat Creek Valley near Cache Creek, British Columbia. The power plant will be situated on elevated terrain in the Trachyte Hills near Harry Lake. Vapor emissions will be released to the atmosphere from evaporative cooling towers, and combustion products from four 500 Mw units making up the plant will be vented from a tall stack. Emissions from the mine will be primarily fugitive dust released from the surface open pits during normal coal removal operations.

The procedural approach or method for this assessment was selected to meet the objectives of the Environmental Report (ER) being prepared. The ER objectives include detailed analyses of:

- sulfur oxides
- nitrogen oxides
- particulate matter
- condensed water droplets
- photochemical oxidants
- meteorological effects
- trace elements

B1.2 APPROACH

The Hat Creek Project air quality assessment considers the distribution of contaminants emitted from the proposed mine and power plant, the production of contaminants by chemical reactions in the atmosphere, and the potential for weather modification effects.

To predict air quality effects of proposed industrial sources, mathematical modeling is well established as a useful tool. The credibility of such simulation techniques is considerably enhanced when the results of on-site field measurement studies are incorporated by the models. While no long-term air quality measurement programs have been performed in the vicinity of the proposed project, several field studies designed to characterize the dispersion meteorology of the Hat Creek Valley area have been conducted. The models used in this air quality assessment have been modified (calibrated) to reflect consideration of these measurements.

The selection of models to estimate air quality effects associated with the various types of emissions from the Hat Creek Project was accomplished as follows: (1) the availability and extent of relevant meteorological input data were reviewed and evaluated; (2) various generic model types were examined for input data requirements and appropriateness of the simulation procedures to the specific characteristics of the project and its environment; (3) the basic models judged to be suitable to provide the information required by the study objectives were tailored to incorporate the results of local measurements. The selected modeling techniques conform to the following fundamental criteria.

- The approach is appropriate in scope and detail for the phenomena to be simulated.
- The accuracy of the approach is balanced by the availability and quality of the input data.
- The results provide an assessment that can be used as a decision-making tool by B.C. Hydro and the public.
- The results are useful for evaluating air quality effects associated with alternative engineering design criteria.

B1.3 SUMMARY OF MODELS

On the basis of the guidelines listed in Section B1.2, four models were selected for use in the air quality assessment of the proposed Hat Creek Project. The applications and general features of these models are summarized in Table B1-1.

The Hat Creek Model (HCM) was chosen to estimate effects of the major power plant emissions on ambient contaminant concentrations in the vicinity of the project site (to a distance of 25 km). The specific contaminants investigated with this model include sulfur dioxide (SO_2), nitrogen dioxide (NO_2), nitric oxide (NO), hydrocarbons (HC), carbon monoxide (CO), and total suspended particulates (TSP). For the local scale calculations, these contaminants are assumed to be unaffected by chemical transformations and physical removal processes. The HCM is an analytical (Gaussian) point-source model that was adapted to include the effects of the severe terrain near Hat Creek and local dispersion characteristics identified in the field studies. Principal attributes of this type of model for application to this assessment follow.

- Ability to simulate plume behavior for a wide range of weather conditions without extensive data manipulations.
- Applicability of the method to investigate air quality effects over all averaging times of interest.
- Adaptability of the results for calculation of expected frequencies of contaminant levels above various thresholds as a function of distance and direction from the power plant.
- Ability to incorporate the effects of terrain on atmospheric transport and diffusion.
- Flexibility of the model, e.g., adaptability to examine feasibility of various air quality control programs.
- Simplicity of approach - errors due to input data and parameterization are readily identifiable.

'Unusual' meteorological conditions that cannot be adequately simulated with the HCM are addressed by interpretation of field measurements.

TABLE B1-1

SUMMARY OF MODELS

Model Name (Acronym)	Contaminants	Geographical Regime	Type
Hat Creek Model (HCM)	Ambient concentrations of TSP, SO_2, CO, HC, NO, NO_2, trace elements from Hat Creek Power Plant	Local	Analytical
	Ambient concentrations and deposition of TSP, SO_2, NO, NO_2, $NO_4^=$ from Hat Creek Power Plant	Regional	
ERT Air Quality Model (ERTAQ)	Ambient concentrations of fugitive TSP, from Hat Creek Mining Activities	Local	Analytical
ERT Cooling Tower Plume Model (COOLTOWR)	Water vapor, visibility reductions, icing, weather modification from Cooling Tower Operation	Local	Numerical
ERT Cooling Tower Drift Model (DEPOT)	Cooling tower drift salts	Local	Analytical/ Empirical

Regional air quality effects of the proposed Hat Creek Project are estimated by a version of the HCM that incorporates methods to calculate concentrations of primary contaminants and those produced by chemical decay (e.g., sulfates [$SO_4^=$]), as well as dry deposition fluxes of SO_2, $SO_4^=$, NO_2, NO, and TSP. The general formulation of the regional model is similar to that of the HCM and is similarly adjusted to reflect on-site measurement data. However, a very conservative terrain assumption is made for the long-range application to ensure that predicted levels are generally overestimated, since there is significantly greater uncertainty in calculating effects for travel distances greater than about 25 km. Models specifically designed to simulate regional transport and dispersion are available, but their validity has been documented primarily in applications for areas with high emission density, extensive air quality measurement data, and numerous meteorological stations. The Hat Creek Project is to be located in a relatively remote region with few major emission sources. Adoption of a sophisticated numerical grid model approach is therefore unwarranted in this case.

Contributions of the proposed coal mining activities to ambient dust (particulate) concentrations were estimated by means of the multi-source Gaussian diffusion model ERTAQ. The ERTAQ formulation is similar to that of the HCM, but can accommodate inputs for any number of point, line, and area sources.

ERT's numerical model COOLTOWR simulates the behavior of saturated cooling tower plumes. This model is an adaptation of techniques originally developed to describe the rise and growth of cumulus clouds. A sophisticated system of thermodynamic algorithms is incorporated to treat moisture phase changes along the plume trajectory, which is determined by simultaneous solution of a set of differential equations describing conservation of plume mass, momentum, buoyancy, total moisture, and entropy. When combined with representative meteorological statistics, the COOLTOWR model can be used to estimate the frequency and extent of tower-induced fogging and icing and obscuration due to elevated visible plumes.

Deposition rates of cooling tower drift salts are predicted by the ERT model DEPOT. This simulation uses inputs characterizing drift emissions; plume trajectories as calculated by COOLTOWR; and representative weather data to predict monthly, seasonal, and annual drift deposition patterns. Both gravitational settling of the larger drift droplets and turbulent diffusion of the smaller ones are accounted for in the DEPOT model. DEPOT is an analytical/empirical model based on a computational scheme developed by J. M. Austin.[1]

All models selected have been successfully implemented for sources similar to Hat Creek and are, therefore, expected to provide a meaningful and reliable assessment of the Hat Creek Project. Calibration procedures using site-specific tracer study results made available by B.C. Hydro are also described in this report.

The effect of photochemical oxidant was not assessed by mathematical modeling because of the complex nature of the chemistry involved, and because a detailed understanding of background conditions is necessary for meaningful simulation. Instead, after a careful method review, it was decided that a qualitative approach based on a literature survey is a suitable procedure to assess this contaminant. This approach is compatible with the assessment guidelines listed in Section B1.2.

Detailed descriptions of the mathematical formulations, input requirements, and assumptions incorporated by the HCM and ERTAQ models are presented in Addenda A and B, respectively. An explanation of the procedures used to calibrate the HCM with results of on-site meteorological and air quality measurements is provided in Addendum C. The cooling tower plume and drift deposition models are described in Appendix D.

B2.0 AVAILABLE DATA BASE

The choice of air quality modeling techniques and the accuracy of the techniques for a given study area are closely tied to the quantity and quality of the existing meteorological data. It is important that the data represent a wide range of possible meteorological conditions to increase the usefulness and representativeness of the model results. Until 1975, the data base for evaluating the air quality of the Hat Creek region was very limited. However, during the past two years, B.C. Hydro has undertaken an intensive measurement program to document the micrometeorology of the Hat Creek region. This section presents summary descriptions of the available meteorological data (see Table B2-1) used to assess Hat Creek air quality. Complete listings of these data sets are provided in Appendix A.

B2.1 INTENSIVE FIELD STUDIES

In 1975, B.C. Hydro authorized a study by the MEP Company to perform measurements to characterize the meteorological conditions of the Hat Creek region during the spring and autumn. This two-part program was conducted in both winter and late summer to obtain data that would reflect typical seasonal meteorological variations.[2,3] B.C. Hydro personnel also participated in both seasonal phases of the field measurement program.

Because the emissions from the proposed Hat Creek Project are to be released from a tall stack, MEP concentrated on obtaining upper air observations during both seasonal phases of the study to determine characteristic vertical profiles of temperature and winds.

Throughout the eight-day spring program, four minisonde releases were made each day from each of four selected locations within the valley system. These releases were made simultaneously, so that an accurate

TABLE B2-1

METEOROLOGICAL DATA SOURCES USED IN MODELING

Source	Period of Record	Type of Data
North American Weather Consultants (Hovind, et al)	2/19/76 - 3/26/76	Oil fog backscatter and SF_6 concentrations, minisondes, pibals, turbulence. Observations conducted during tests.
(Hovind, et al)	7/31/76 - 8/11/76	Oil fog backscatter and SF_6 concentrations, minisondes, pibals, turbulence. Observations conducted during tests.
MEP Project (Weisman, et al)	3/1/75 - 3/11/75	Minisondes, pibals, constant level balloons. Observations conducted four times daily.
(Weisman, et al)	8/31/75 - 9/11/75	Minisondes, pibals, constant level blloons. Observations conducted four or nine times daily.
B.C. Hydro	1/1/75 - 12/31/75	Surface observations consisting of wind speed and direction, temperature, humidity. Hourly sequential observations.
Atmospheric Environment Service of Canada	1/1/75 - 12/31/75	Radiosondes from Vernon, Prince George, and Port Hardy. Observations conducted two times daily.
	1/1/75 - 12/31/75	Surface observations of wind speed, wind direction, and cloud cover at Kamloops.
	1/1/75 - 12/31/75	Surface wind field observations from Ashcroft, Williams Lake, and Kelowna.

description of the distributions of vertical temperature profiles and associated vertical wind fields could be obtained. The observation program was modified during September to include nine soundings per day at two of the sites.

Data from seven mechanical weather stations, located in and around Hat Creek Valley and operated by B.C. Hydro, were available to MEP personnel. Also, four hygrothermographs were situated on the southwest-facing slopes of the Hat Creek Valley. These surface data, in conjunction with the minisonde soundings, were used to identify diurnal variations of the vertical temperature profile, surface along-valley and cross-valley drainage flows, and upslope circulations due to daytime heating effects.

MEP also conducted a series of constant-level balloon flights to identify flow streamline characteristics within the valley. These experiments included a series of timed releases to obtain statistical dispersion information.

Under sponsorship by B.C. Hydro, North American Weather Consultants (NAWC) conducted an airborne tracer study during the winter and summer months of 1976 (Hovind et al.).[4] B.C. Hydro personnel also participated extensively in this program. This program consisted of gas tracer releases from an aircraft to simulate emissions at the effective height of release at two proposed plant sites within the valley complex. The tracer plumes were tracked by an instrumented aircraft, which made transects through the plumes at various altitudes and distances from the release point. A surface array of samplers was operated in conjunction with the airborne sampling program to determine ground-level concentrations due to expected emissions.

Data obtained during the tracer studies reflect the fact that the experiments were performed with the objective of documenting plume behavior under suspected worst-case dispersion conditions. Thus, it is not possible to rely solely on these measurements for analyses requiring consideration of diffusion over long time periods and/or a spectrum of meteorological

conditions. Rather the field study provided detailed data for a number of selected weather conditions that could be related to classification schemes based on more routinely available information. In this regard, the gas tracer study results were invaluable in the formulation of site-specific modeling techniques.

NAWC and B.C. Hydro also conducted a series of pilot balloon releases during both seasonal phases of the program. The wind data from these observations, coupled with minisonde releases made during the hours centered around the plume sampling tests, provide a picture of the vertical wind and temperature structures within and above the valley on the days that plume samples were taken.

B2.2 SURFACE DATA NETWORK

B.C. Hydro operates eight mechanical weather stations located at various sites throughout the region (see Figure B2-1). Data from these stations were used during the MEP project. These eight stations provide wind, temperature, and humidity data on a continuous basis. Surface wind field data collected by the Atmospheric Environment Service (AES) of Canada are also available from Ashcroft, Kamloops, Williams Lake, and Kelowna, and were used with the surface data from the B.C. Hydro network in performing the model calculations for power plant and cooling tower emissions. A wind rose was constructed from the Kamloops data to examine air quality effects due to the industrial sources in that area.

B2.3 UPPER AIR OBSERVATIONS

Radiosonde observations conducted by AES are available from Vernon, Prince George, and Port Hardy. A review of the upper air data reveals that temperature profiles collected at Vernon are most representative of the Hat Creek Project area. These data have been used in conjunction with MEP data to identify characteristic mixing depths that would occur in the Hat Creek region. The Vernon data were used to create a wind rose used to calculate annual average contaminant concentrations due to the Hat Creek Plant on a regional scale.

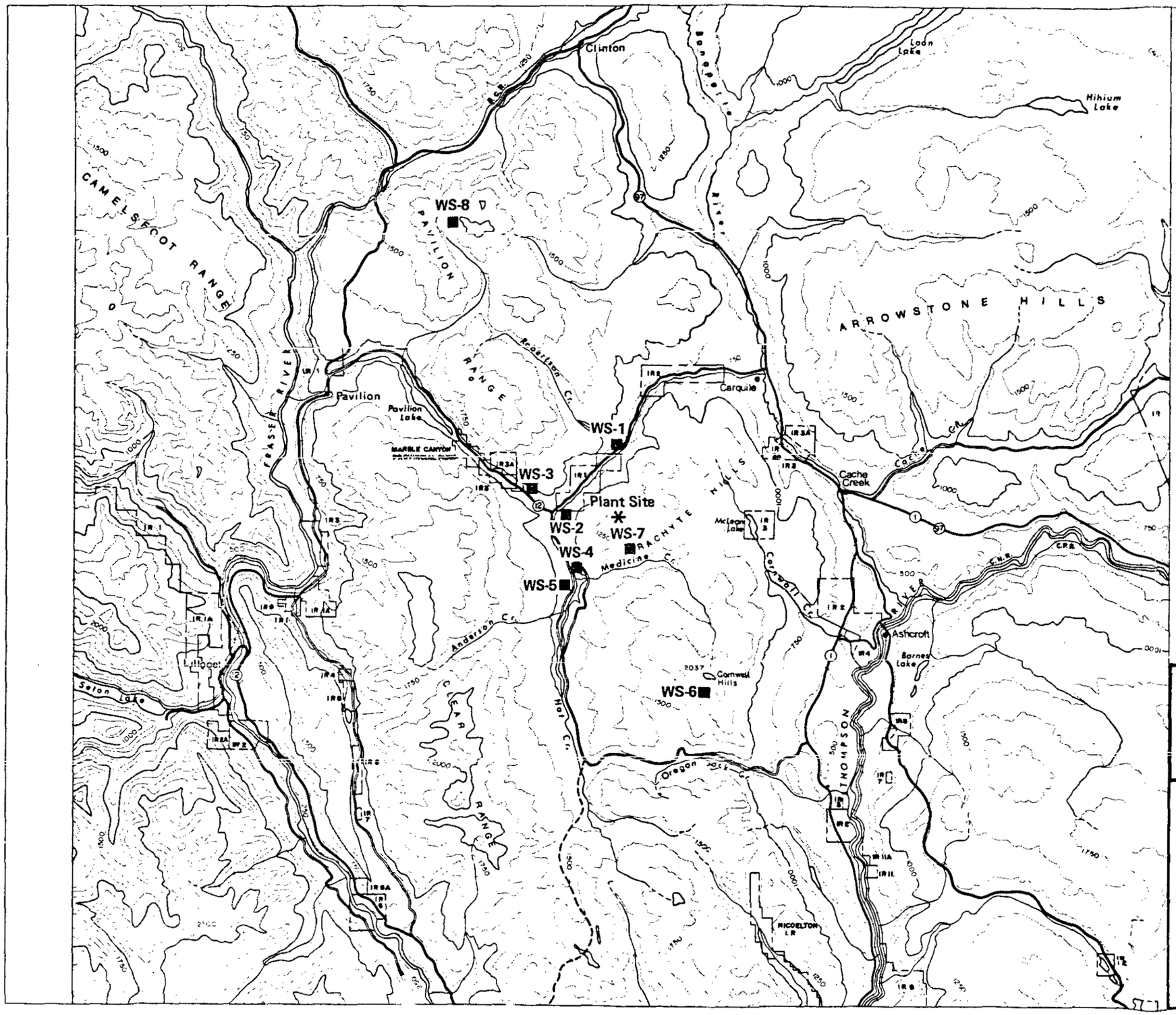

SCALE - 1:250,000

5 0 Kilometres 5 10 15

CONTOUR INTERVAL - 250 METRES

BRITISH COLUMBIA HYDRO AND POWER AUTHORITY
HAT CREEK PROJECT

DETAILED ENVIRONMENTAL STUDIES

Figure B2-1 Locations of the B.C.Hydro Mechanical Weather Stations in the Hat Creek Area

80.4276

B3.0 MODEL METHOD REVIEW

The accuracy of air quality model predictions for a given application depends, in large part, on the extent and representativeness of available baseline data, physical characteristics of the study area, the configuration of sources to be considered, and the ability of the selected simulation techniques to accomodate these site-specific factors. Very sophisticated methods may not improve the accuracy of predictions for applications unless very extensive data are available, and where many assumptions must be made to satisfy input requirements.

Many types of models designed to estimate effects of stack emissions, mining activities, and cooling tower effluents are available. Reviews of such models have been reported in the recent literature by several investigators, e.g., Eschenroeder[6] and Roth et al.[7], and will not be repeated here. In this section, various generic modeling methods that have been considered for use in the Hat Creek assessment are discussed, and the important factors determining the appropriateness of each model type are identified.

B3.1 ANALYTICAL METHODS

Most mathematical treatments of the advection and diffusion of passive contaminants in the atmosphere involve solutions to a basic equation expressing mass conservation within a parcel of air:

$$\frac{\partial C}{\partial t} + \bar{V} \cdot \nabla C = \nabla \cdot (K \nabla C) + S \qquad \text{(B3-1)}$$

where

C is concentration of material in the parcel,

$\bar{V}$ is the wind vector,

K is the turbulent diffusivity, and

S is source strength.

Probably the best-known exact (analytical) solution to Equation B3-1 is the steady-state Gaussian solution. A number of models have been developed for applications where the basic assumptions of the Gaussian formulation are approximately valid. These assumptions are that:

- the distributions of contaminant mass in the vertical and cross-wind directions are well-approximated by normal (Gaussian) curves;
- meteorological conditions are steady-state, i.e., wind and eddy diffusivity are constant during the period represented by each calculation;
- contaminant plume mass is conserved; and
- downwind distance is large compared with plume, i.e., width; this is far field approximation.

Because analytical models are based on algebraic equations, they are easily applied, and the results may be readily interpreted for physical consistency. Such models ordinarily require only routinely available input data and have modest computing requirements. However, many simplifying assumptions regarding the behavior of the atmosphere are inherent in their use, with corresponding restrictions on the applicability of the results. Thus, while analytical dispersion models are attractive for their simplicity of formulation and use, they may, in some circumstances, provide a limited representation of atmospheric processes. Certain site-specific characteristics of transport and diffusion must be evaluated for available measurement data.

Basic input requirements for Gaussian models generally consist of elementary source emission properties, wind speed, wind direction, atmospheric stability, and mixing height at a single representative location. Model predictions are applicable to short averaging times, ten minutes to an hour, but can be generalized for longer periods by the use of sequential or statistical meteorological inputs. Terrain effects may be simulated within an analytical framework by incorporating surface elevation data and modifying plume rise and/or dispersion rate parameterizations.

Analytical models generally can accommodate only steady, two-dimensional wind fields. They cannot be used to simulate diffusion and transport processes during periods characterized by changing winds or geographically inhomogeneous turbulence due to irregular solar heating. They are unable to treat complex phenomena such as stagnation or plume direction reversal due to vertical wind shear. Analytical methods are generally limited in their ability to treat simultaneous dynamic and chemical processes. However, as described in Section B4.2, solutions to Equation B3-1 that include linear chemical transformation and modified surface boundary conditions to simulate deposition are available.

B3.2 NUMERICAL METHODS

Computer schemes involving numerical solutions to the basic diffusion equation are less frequently used than analytical models. Numerical models are generally more powerful, in that complex circulation patterns and chemical processes can be simulated. However, implicit in these features is the requirement for detailed input information. Thus, for applications involving remote sources where such data are unavailable, simpler modeling techniques may be preferable. For example, numerical models that simulate geographical and/or temporal wind and diffusivity changes are readily available. But for a location such as Hat Creek, data adequate to document such effects at the expected height of the power plant plume do not exist. Improved resolution of the vertical structure of the lower atmosphere near the power plant site will become available through measurements on a 100m meteorological tower to be installed well in advance of plant operation (see Appendix H). Use of a numerical dispersion model in this case would involve incorporation of a number of assumptions and approximations just to derive a meteorological input package for a single simulation. Errors inherent in the model itself would compound the uncertainty of the results. In general, trade-offs between the degree of detail in the input specifications and the corresponding expected improvements in the prediction accuracy must be weighed; a considerable amount of time can be spent in preparing

inputs in the form required by sophisticated numerical diffusion models. Furthermore, computing costs are often substantially greater for numerical models.

Numerical techniques do, however, offer practical benefits for simulating the complex thermodynamic and aerodynamic mechanisms governing the behavior of saturated vapor plumes discharged from cooling towers. In addition, the effects of cooling towers are largely localized, such that the extensive data requirements of numerical models for regional scale simulations are not applicable. Observations of wind speed and direction, temperature, humidity, and stability in a location representative of conditions at the plant site are sufficient meteorological inputs for cooling tower simulations. Analytical treatments, e.g., Gaussian formulations patterned after diffusion models for inert stack gas emissions, generally do not incorporate routines to handle water phase changes within the plumes. Since it is these phase changes that determine whether the plumes are visible, an analysis of potential fogging, icing, and obscuration due to cooling tower plumes is best accomplished with numerical modeling techniques. Models for this purpose with relatively simple meteorological input requirements and reasonable computing costs are available.

B3.3 SUMMARY OF MODEL REVIEW

The discussion presented in this section indicates that a number of air quality models are available for use in estimating air quality effects due to emissions of the proposed Hat Creek Project. Relevant features of analytical and numerical models are summarized in Table B3-1. Certain model types offer clear advantages for specific applications, but the selection of modeling techniques to predict contaminant effects due to the power plant and mine remains dependent on the availability of meteorological data, the source characteristics of the facilities, and the principal objectives of the model analyses. The following sections provide descriptions of the models selected for use in the Hat Creek assessment.

TABLE B3-1

GENERIC AIR QUALITY MODEL DESCRIPTIONS

Type of Emissions	Model Type	Meteorological Inputs	Relative Cost to Use	Time Scales Simulated	Geographical Scales Considered
Power plant stack and mining activities	(a) Analytical (Gaussian)	Wind speed and direction, stability, mixing depth at one location sequential or statistical input can be accommodated.	Low	10 minutes to 1 hour (longer times with sequential inputs).	Local (<25 km) Larger scales with appropriate modifications.
	(b) Numerical (finite difference)	Horizontal wind speed and direction, vertical wind speed and direction, diffusivities, mixing depths at all grid points as a function of time.	High	Flexible (computing costs escalate rapidly time scale).	Local or regional.
Cooling towers	(c) Analytical (Gaussian)	Same as (a).	Low	Same as (a).	Local only.
	(d) Numerical	Same as (a).	Moderate	Hourly, monthly, seasonal, annual depending on meteorological input form.	Local or regional.

B4.0 MODELS FOR THE POWER PLANT AND COAL MINE

Discussions in previous sections have identified practical constraints bearing upon the types of modeling techniques that should be used in the Hat Creek air quality assessment. The specific models selected to estimate local and regional effects due to gaseous and particulate emissions from the power plant stack and fugitive dust from mining activities are described in this section. Section B4.1 provides a description of the Hat Creek Model (HCM), which was used to predict concentrations of stack gas contaminants. The adaptation of the HCM to estimate regional-scale effects of these emissisons is discussed in Section B4.2. The ERT Air Quality Model (ERTAQ), used to calculate incremental effects attributable to mining activities and to other industrial sources in the study region, is described in Section B4.3. Finally, in Section B4.4 the methods by which the basic diffusion model results were analyzed in terms of alternative air quality control systems are presented.

B4.1 THE HAT CREEK MODEL

The fundamental expression chosen for calculation of ground-level contaminant concentrations from the stack of the proposed power plant is the Gaussian plume equation. The basic model was modified to accommodate inputs appropriate to the rugged terrain surrounding the plant site and dispersion characteristics inferred from on-site meteorological measurements. The most important assumptions incorporated by the HCM for application to this study are:

- wind speed and direction in the vicinity of the stack remain constant at the hourly average values for each hour;
- the plume rises from the stack exit due to its excess buoyancy to an equilibrium height that is well approximated by the equations of Briggs;[8]

- at any downwind distance, the maximum concentration is found on the plume centerline; plume concentrations decrease away from the centerline in the cross-wind and vertical directions according to normal (Gaussian) distributions;
- the Gaussian crosswind and vertical plume concentration profiles represent hourly-average properties; and
- the stack emission rate is constant and meteorological parameters determining plume geometry are constant (i.e., the model assumes steady-state conditions during each computation of hourly concentrations).

Calculation of ground-level concentrations requires that the model simulate a number of atmospheric processes governing plume behavior, including:

- Transport by the mean wind
- Dispersion by turbulent eddies
- Buoyant plume rise
- Terrain effects

(a) Transport and Dispersion

The HCM formulation assumes that the stack plume centerline for each hour of input data is aligned with the mean wind during that period. Material in the plume is transported horizontally downwind at the mean wind speed. Plume material is considered to be distributed normally about the centerline in the cross-wind and vertical directions by turbulent eddy motions. The atmosphere, being a continuous, fluid medium, exhibits an infinite number of states, each with its own turbulence characteristics. The primary emphasis in dispersion modeling development in recent years has been toward categorization of turbulence properties (which are difficult to measure directly) for routinely measured meteorological variables. In the Gaussian model, turbulence is parameterized in terms of the dispersion coefficients σ_y and σ_z, which

are respectively, the standard deviations of plume mass distributions in the cross-wind and vertical directions. The turbulence typing scheme incorporated by the HCM is based on measurement results obtained at Brookhaven National Laboratory by Smith[9] and interpreted to provide curves of σ_y and σ_z as functions of plume downwind travel distance and atmospheric stability (ASME[10]). The formulations for σ_y and σ_z employed in the HCM are similar to those of Smith[9] but were modified to reflect the results of on-site field studies. Addendum C presents a description of the HCM calibration procedures.

The calibration analysis derived from the North American Weather Consultants (NAWC)[4] measurements in Hat Creek Valley indicates that horizontal plume dispersion (as characterized by σ_y) in the Hat Creek area is greatest during light-wind conditions. For each stability category, it was found that σ_y as a function of travel distance (x) can be approximated by the expression $\sigma_y = ax^b$. Table B4-1 lists the values of 'a' and 'b'.

Vertical dispersion of the tracer gas plumes released by NAWC was found to be governed primarily by the vertical temperature profile (lapse rate). Values of 'c' and 'd' used to calculate $\sigma_z = cx^d$ for the HCM are also listed in Table B4-1.

(b) Plume Rise

A frequently used scheme for estimating the rise of buoyant plumes from stack sources was developed by Briggs[8]. The Briggs plume rise formulae have been validated for a number of data sets; however, previous experience and applications involved sources with smaller initial buoyancy flux than that expected for the Hat Creek Plant. In a personal communication Briggs[11] indicated that the theoretical basis for his plume rise equations should be applicable to any stack plume. However, the atmospheric temperature structure above the tall stack proposed for the Hat Creek Plant may be different from the conditions under which the Briggs formulae have been validated. In the absence of additional information to support this observation, the Briggs plume rise equations have been selected as the best available approximation.

TABLE B4-1

DISPERSION COEFFICIENTS DEVELOPED FOR THE HAT CREEK MODEL

Lapse Rate (γ) Category $^{o}C/100$ m	Wind Speed* (WS) Category (meters/sec)	Horizontal Dispersion Coefficients a	b
γ less than -1.5 (unstable)	WS less than 2.0	0.40	0.91
γ greater than -1.5 (neutral, stable)	WS less than 2.0	0.36	0.86
γ less than -1.5 (unstable)	WS greater than 2.0	0.36	0.86
γ greater than -1.5 (neutral, stable)	WS greater than 2.0	0.32	0.78

Lapse Rate (γ) Category	Wind Speed (WS) Category	Vertical Dispersion Coefficients c	d
γ less than -1.5 (unstable)	WS less than 2.0	0.40	0.91
γ less than -1.5 (unstable)	WS greater than 2.0	0.33	0.86
γ greater than -1.5 (neutral, stable)	any	0.22	0.78

*Wind speed measured at plume height.

The preliminary design of the Hat Creek stack specifies that effluent from the four (500 Mw) boiler units will be exhausted through four flues contained within a single common casing. Thus, plume rise from the stack is computed in the HCM as if the four units were exhausted through an equivalent single flue. It is known, e.g., see Bosanquet[12] et al., that the aggregate rise of plumes from multiple stacks is greater than would be expected from any one of the stacks alone, but less than that from a single equivalent source with the combined buoyancies of all the stacks. However, the separation between the four proposed flues of the Hat Creek stack is very small, such that any reduction of rise due to this factor is considered negligible.

(c) Terrain Effects

The HCM simulates the effect of transport over elevated terrain during neutral and unstable atmospheric conditions by allowing the plume to be lifted one-half of the difference between the terrain elevation and the stack base elevation. This treatment is based on potential flow theory. It has been found by Egan[13] that a plume from an elevated source upwind of a terrain feature will approach terrain most closely at the crest. The height of approach can be calculated under certain simple conditions. Above the crest the streamline spacing in the vertical dimension will be less than that expected over valleys or level terrain. The resulting effects are increased wind speed at the crest and reduced vertical spread of the plume. Implementation of a 50% (or half-height) correction is equivalent to incorporation of the combined effects of increased wind speed and modified plume spread expected from theoretical arguments for neutral stability. In the HCM the 50% correction is assumed for neutral and unstable conditions.

An elevated plume of gases will approach terrain features more closely, however, during stable conditions. The distance of closest approach can be computed for simple situations when the terrain feature can be assumed to be two-dimensional; for example, an infinitely long ridge. In this case, Queney et al.[14] have demonstrated that a plume is lifted about 20

to 40% of the terrain elevation during stable flows. The exact percentage depends on the original height of the plume upwind of the crest.

There is no exact solution to the problem of stable air flow over irregularily shaped features. Experimental and theoretical evidence, e.g., Egan,[13] indicates that a plume should approach closer to three-dimensional features than to two-dimensional features by about a factor of two. For example, a plume would travel about half as far above an isolated peak as over a long ridge. During stable conditions the effect of elevated terrain is simulated in the HCM by allowing the plume to be lifted a vertical distance equivalent to 10% of the difference between the terrain and stack base elevations. A 10% terrain correction represents a reasonable (yet conservative) simulation estimate.

In summary, for all stabilities and wind speeds the model allows the plume to approach a terrain obstacle without allowing direct plume impaction. The distance of approach and height above the terrain is stability dependent.

(d) Model Averaging Times

The HCM was used to calculate ground-level contaminant concentrations within 25 km from the proposed power plant site. It is assumed that plume travel times to points within this distance are short enough so that depletion of stack gases by chemical transformations or deposition processes may be neglected. A one-year sequence of hourly centerline concentrations was computed with meteorological input data from the B.C. Hydro mechanical weather stations (see Section B2.3). Multiple-hour averages were formed from the hourly values. Three-hour concentrations were calculated by averaging consecutive hourly centerline values, except during light wind/stable periods. Simple averaging of centerline values was considered unduly conservative for these conditions, which are characterized by pronounced wind directional variability. Justification for this conclusion is given by Wilson et al.[15] and Lague.[16]

For these periods, the plume mass is considered to be distributed uniformly across a 22.5° sector centered along the mean wind direction. This sector-averaging assumption is used in computing concentrations for averaging times greater than three hours regardless of weather conditions. One-hour, 3-hour, 8-hour, 24-hour, seasonal, and annual average concentrations during the 1-year period (1975) were calculated with the HCM and analyzed for various air quality control systems.

(e) Sulfur Dioxide Control Systems

The HCM was used to evaluate incremental air quality effects of stack emissions from the proposed power plant with and without selected SO_2 control systems. Both flue gas desulfurization (FGD) by means of wet scrubbers and meteorological control systems (MCS) were examined from the standpoint of achieving specified ambient SO_2 levels in the vicinity of the Hat Creek Project. The following specific SO_2 control strategies were examined in detail: (1) FGD with a 366m stack; (2) MCS with a 366m stack; and (3) MSC with a 244m stack.

An FGD system designed to reduce SO_2 emissions by 54% was examined by the HCM, using the sequential meteorological inputs from the mechanical weather stations and emission characteristics corresponding to full-load operation with scrubbers. The analysis procedure included predictions of concentrations for averaging times from one hour to one year. Results were statistically analyzed to estimate expected frequencies of concentrations above various threshold values as a function of distance and direction from the plant site.

An MCS is a systematic plan of defined procedures for the reduction of contaminant emissions in response to observed or predicted meteorological conditions associated with relatively high ambient concentrations. Such a program involves the specification of control measures to be taken intermittently as required by the dispersion characteristics of the local atmosphere. For the Hat Creek assessment, the MCS was considered to involve:

- use of 0.45% sulfur coal when atmospheric conditions are favorable for contaminant dispersion;

- use of 0.21% sulfur coal when atmospheric conditions are such that use of 0.45% sulfur coal would lead to SO_2 levels above assumed guideline values. This control action would be used during the winter months (November through February) when, it is assumed, demand on electrical generation by the Hat Creek facility would be the greatest; and

- uniform load reduction of the four 500-Mw generating units (without changing fuel) during periods characterized by atmospheric conditions capable of producing SO_2 concentrations above the guideline values with full-load operation. This control action would be preferred over fuel switching during the months March through October, when the demand for electric power is generally less than available reserves.

Air quality effects of load reduction were investigated by direct application of the HCM with emissions adjusted to reflect discrete partial load conditions. Evaluation of expected fuel switching requirements during winter months was accomplished by a computer analysis program designed for this purpose. This program, the DECA model, is described in Appendix C. DECA uses results of the HCM to predict the frequency and duration of required fuel switch actions to maintain SO_2 levels below specified threshold values.

A complete description of analysis methods and results of the SO_2 control system assessment is provided as Appendix C.

B4.2 THE REGIONAL DISPERSION MODEL

Air quality effects of power plant emissions at locations between 25 and 100 km from the proposed Hat Creek Project were estimated by an adaptation of the HCM. While the Gaussian formulation is not generally intended for regional-scale applications, the low density of meteorological and air quality monitoring stations in the project area favors

adoption of a relatively simple modeling approach. To compensate for the uncertainty associated with application of the Gaussian model for regional scale calculations, model input parameters were selected to ensure that conservative predictions would result, i.e., errors in the calculated concentrations tend to be in the direction of overestimates.

The regional model incorporates algorithms to simulate simple chemical transformation and dry deposition processes, since such mechanisms may be significant over larger travel distances. Oxidation of SO_2 to produce $SO_4^=$ is assumed to proceed at a rate of one percent per hour (Hidy et al.).[17] Deposition of contaminants is calculated as a flux at the ground surface. A technical description of the regional model is provided in Addendum A.

Seasonal and annual average concentrations and deposition rates of SO_2, $SO_4^=$, NO, NO_2, and TSP attributable to the proposed power plant were estimated by the regional model. Meteorological inputs consisted of an annual wind rose developed from 700mb winds measured twice daily at Vernon, B.C. The average elevation of this pressure surface is about 3000m (10,000 ft) MSL, and is near the expected final height of the Hat Creek plume. Use of wind data taken at 12-hour intervals is adequate to compute seasonal and annual average concentrations and deposition rates.

As noted above, uncertainties inherent in the use of mathematical modeling for a regional assessment require that conservative assumptions be incorporated in the input data. For this reason, terrain elevations corresponding to the model receptor points were assigned elevations as follows: (1) for receptors located at elevations below that of the proposed stack base (about 1400m or 4,650 ft), the elevation was set at the stack base height; (2) receptors at elevations above the stack base, were assigned their actual values. This input specification is equivalent to placing the 'ground' plane at the stack base elevation and results in a predicted plume approach height much nearer to the terrain than would actually be expected in valleys downwind from the plant. As a result, ground-level concentrations are probably overestimated.

B4.3 THE ERTAQ MODEL

The ERTAQ diffusion model is a Gaussian formulation similar to the HCM for input requirements, assumptions, and mathematical representation. However, ERTAQ accommodates multiple-source data and is, therefore, appropriate for estimating combined air quality effects due to a number of emission sources. In the context of the present analysis, this model is used to evaluate TSP concentrations from Hat Creek coal mining activities. A detailed technical description of the ERTAQ model is provided in Addendum B.

Fugitive emissions related to mining activities are input to the model as point, area, and line sources. Operations classified as point sources include the action of trucks dumping coal at transfer points; line sources consist of vehicle operations over unpaved roads and the maintenance and construction of haul roads; the major pit operations (shoveling, scraping, and blasting) as well as emissions from coal piles and wind erosion from unprotected areas are classified as area sources.

A stability wind rose constructed from surface meteorological measurements at the B.C. Hydro mechanical weather station No. 5 (see Figure B2-1) was used to predict annual average particulate concentrations due to fugitive dust emissions at the mine. Worst-case 24-hour values within the Hat Creek Valley were also estimated using the ERTAQ model. Emission factors incorporate assumptions regarding the amount of emitted material that remains suspended without being deposited by gravitational settling. ERTAQ cannot account for the fact that the principal mining operations will occur within the pit and will not generally escape to affect particulate concentrations beyond this area. Thus, concentrations beyond a few hundred meters from the mine are expected to be overestimated in the predictions.

B5.0 COOLING TOWER MODELS

ERT's numerical model COOLTOWR simulates the complex thermodynamic and aerodynamic processes governing the behavior of moist, buoyant plumes introduced to the atmosphere. A second model, DEPOT, estimates the geographical distribution of cooling tower drift deposition. Special adaptations of both models have been developed to produce realistic predictions of potential effects associated with operation of rectangular mechanical draft, round mechanical draft, and hyperbolic natural draft tower systems. The following subsections include brief technical descriptions of these models and explanations of the approach adopted by ERT in employing them to simulate potential effects due to atmospheric emissions resulting from operation of various types of cooling towers in the Hat Creek region. Detailed descriptions of the COOLTOWR and DEPOT models are presented as Addenda to Appendix D.

B5.1 MODEL DESCRIPTIONS

COOLTOWR is a numerical model that calculates the physical properties of moist plumes as a function of downwind distance from the cooling towers. The model is designed to provide simultaneous solutions to a system of differential equations describing the conservation of plume mass, total plume moisture, plume momentum, and plume specific entropy. A series of thermodynamic routines is included to simulate phase changes of plume water along the trajectory of the cooling tower effluent. The principal assumptions in COOLTOWR are: (1) plume mass flux increases with downwind distance according to the rate at which ambient air is entrained; (2) changes in the plume's vertical momentum are due to its buoyancy relative to the environment; (3) horizontal momentum of the plume mass depends only on the rate of entrainment induced by its motion relative to the wind; (4) total plume moisture flux increases along its trajectory with the rate at which ambient water vapor is entrained; (5) the

depletion of plume moisture due to precipitation is negligible; and (6) thermal energy in the plume at any point in its trajectory is the sum of its initial heat content and that of entrained air.

The DEPOT model uses plume trajectories computed by COOLTOWR to simulate the processes by which drift droplets (specified in terms of an initial mass-size distribution) undergo transport and dispersion in the atmosphere. As large droplets fall from the saturated plumes into the unsaturated atmosphere, evaporation reduces their diameters and, therefore, their fall velocities. DEPOT accounts for these complex processes governing the behavior of drift in the atmosphere. As with COOLTOWR, special features are incorporated by DEPOT to distinguish between the source characteristics of various cooling tower designs.

B5.2 TECHNICAL APPROACH

Because the plume of a cooling tower is composed of water droplets and water vapor, the behavior and effects of the plume will differ somewhat from those of a contaminant gas plume. COOLTOWR and DEPOT are specifically designed to treat the following environmental effects associated with cooling tower plumes:

- obscuration or shadowing by elevated visible (saturated) plumes
- surface icing and foggings
- multiple tower effects
- salt deposition due to cooling tower drift
- plume downwash

(a) Visible Plume Length

In practice, the plume remains visible (due to the scattering of light) only so long as it contains droplets of condensed water of sufficient size and number to make the plume substantially opaque. Otherwise, the plume may not be visible even though it contains small amounts of the

condensate. In the present model, based on the relation between horizontal visibility and the liquid water content given by Houghton and Radford[18] it is assumed that the plume is invisible if the condensate mixing ratio (r_c) falls below 0.00001. The maximum visible plume length is calculated directly from the model as the horizontal distance at which $r_c = 0.00001$.

(b) Icing and Fogging

Most fogging and/or icing incidents will occur near the cooling towers as a result of aerodynamic downwash (especially for mechanical draft towers). However, to account for the elevated terrain surrounding the proposed power plant site, the results of plume rise and transport calculations were superimposed upon the terrain features. At those points where the terrain intercepts the plume, fogging or icing (depending on the ambient temperature) will occur. As explained in the discussion of cooling tower modeling results, such effects due to impingement of extended visible plumes at high elevations are predicted to occur only about five hours per year.

(c) Multiple Tower Effects

The behavior of combined plumes from a row of identical cooling towers is simulated by a sub-model of the COOLTOWR program. Geometrical criteria are used to determine points of intersection of individual plumes. Then, physically realistic assumptions are used to describe alterations in plume properties (e.g., fluxes of its mass, total moisture, and momentum) resulting from the merging process. At the point of merging, the properties of the mixed plumes are combined in the model. The merging scheme is generalized to allow simulation of plume behavior from a row of any number of cooling towers.

(d) Salt Deposition Due to Cooling Tower Drift

While condensation products such as cooling tower fog are reasonably pure water, drift droplets have the composition of the circulating water. Through evaporation and the addition of makeup water, salt concentrations higher than those found in the source water occur in the circulating water after a few cycles through the condensers. Chemicals present in the circulating water can therefore be deposited on the countryside by the drift. The drift is carried aloft in the plume as long as the upward motion of the plume is greater than the settling velocity of the droplet. Droplets are eventually deposited on the ground at various downwind distances that are determined by the wind speed and the mass-size distribution of the drift escaping the towers.

The DEPOT model uses inputs from COOLTOWR and drift emission characteristics to describe mean trajectories for each of a range of drop sizes. Larger droplets reach the ground by gravitational free-fall; smaller drops by a combination of settling and motions corresponding to turbulent atmospheric eddies. Monthly, seasonal, and annual average deposition patterns are computed by summing the contributions of all drop sizes and incorporating meteorological joint-frequency statistics.

(e) Plume Downwash

During strong crosswinds, aerodynamic downwash of cooling tower plumes can occur unless the initial vertical momentum and/or buoyancy is sufficient to carry it beyond the region of flow separation in the lee wake of the tower. Hyperbolic natural draft towers are massive structures, presenting substantial obstructions to local winds and producing some lee downwash. The height of such towers (122m to 152m), however, is sufficient to preclude a resulting plume impact at the ground in regions of flat terrain. Fogging at points located on topographic features above the tower site may occur. Round mechanical draft towers also exhibit favorable downwash and recirculation characteristics. Plumes from such towers behave essentially like those from a small natural draft tower. The symmetry of both designs makes the behavior of the

plumes independent of wind direction. For applications involving natural draft and round mechanical draft towers, the COOLTOWR model employs a downwash criterion derived from results obtained by analysis of observational data by Overkamp and Hoult.[21] The critical ratio of plume velocity to wind speed required to produce downwash is determined as a function of the plume Froude number.

The occurrence of downwash from a rectangular mechanical draft tower is dependent upon the relative angle of the wind to the tower. This tower design is conducive to ground level plume impacts, i.e., icing and fogging. The expression advocated by Hanna[22] to describe the deflection of rectangular tower plumes during downwash conditions is incorporated by COOLTOWR.

B5.3 MODEL ADAPTATION

For application to the B.C. Hydro cooling tower simulation analysis, the COOLTOWR model incorporates expressions for plume growth rate (dispersion coefficients) consistent with those derived from on-site data as described in Section B4.2. In addition, vertical wind speed profiles determined from local meteorological data are used as model input. The results of measurement studies by Slawson et al.[19] and Meyer et al.[20] in the vicinity of operational cooling towers are also used to determine appropriate entrainment coefficients for both mechanical draft and natural draft tower designs.

Slawson et al.[19] observed time-mean trajectories of plumes from the three natural draft cooling towers at the Tennessee Valley Authority's Paradise Stream Plant. Meyer et al.[20] presented extensive data (collected during the fall and winter of 1973-74) of the visible plume from rectangular mechanical draft cooling towers at the Potomac Electric Power Company's Benning Road generating station in Washington, D.C., where 16 tower cells serve fossil-fuel units with a total of 560 Mw capacity. These well-planned and documented observations have been used to determine entrainment coefficients to describe the growth of multiple-cell plumes from rectangular mechanical draft cooling towers. Similarly, the observations of Slawson et al.[19] were used for the calibration of the COOLTOWR model for application to natural draft towers.

B5.4 MODEL APPLICATIONS

The investigation of potential environmental effects associated with cooling tower operation at B.C. Hydro's proposed Hat Creek Plant involves the following specific modeling tasks:

1) incremental effects upon the frequency of local ground fog formation due to the interception of visible plumes with the ground, and the locations where such effects are significant;

2) the frequency of tower-induced icing initiated at or near the ground as a result of contact with saturated plumes during sub-freezing ambient conditions;

3) the extent of atmospheric obscuration attributable to persistent elevated cooling tower plumes, including the geographical distribution of such plumes during typical monthly and annual periods;

4) the extent of icing directly attributable to seasonal water drift accumulations resulting from cooling tower operation; and

5) the airborne drift concentrations, the patterns of ground-level salt drift deposition, and potential effects on nearby sensitive locations.

B6.0 OTHER ASSESSMENT METHODS

Previous sections of this Appendix have dealt with modeling techniques used to evaluate specific air quality effects of the Hat Creek Project. Some potentially important issues, however, do not lend themselves to analysis by such formal mathematical procedures because of insufficient data, incomplete understanding of the governing processes, or limitations of present prediction tools. Four such subjects are discussed in this section. These include the effects of the project on:

- visibility degradation;
- precipitation acidity;
- ambient levels of photochemical oxidant; and
- ambient levels of secondary nitrogen oxides.

Information from the technical literature formed the basis for evaluation of these effects. The rationale and technical considerations involved in the selection of assessment methods for treating the four topics are presented in the following subsections.

B6.1 VISIBILITY DEGRADATION

Visibility and visual range are potentially affected by emissions of atmospheric contaminants. Visibility, as used in this report, refers to the clarity with which an object stands out from its surroundings; visual range is the distance at which an ideal black object can just be seen against the horizon.

In the western part of North America, there are many areas located at great distances from any major sources of anthropogenic aerosols. In these areas, visibility and visual range are largely governed by light scattering of particulates and aerosols from natural sources. Thuiller et al.[23] have computed that the visual range for such locations can be greater than 160 km. In these areas, a small increase in the density of light-scattering particles could greatly affect the visibility of objects in the area of an observer.

Much of the work done by researchers investigating aerosol effects on visibility is based on light-scattering theory developed by Koschmieder.[24] In his work, Koschmieder derived a relationship between the light scattering or extinction coefficient and visual range. For the human eye with a minimum brightness contrast of 0.02, and for a light wavelength of 550 nm (the wavelength at which the human eye is most sensitive), the relationship can be expressed as:

$$L_V = \frac{\ln 0.02}{b} \qquad \text{(B6-1)}$$

where

L_V is the visual range (meters); and

b is the scattering extinction coefficient.[25]

The extinction coefficient can be described as the sum of several components:

$$b = b_{scat} + b_{Rayleigh} + b_{abs\text{-}gas} + b_{abs\text{-}aerosol}$$

where

b_{scat} is the component due to aerosol scattering;

$b_{Rayleigh}$ is the scattering due to air molecules;

$b_{abs\text{-}gas}$ accounts for absorption due to gases; and

$b_{abs\text{-}aerosol}$ for the absorption due to particles.

In most cases, the $b_{abs\text{-}gas}$ and $b_{abs\text{-}aerosol}$ are negligible and b_{scat} is much greater than $b_{Rayleigh}$ for contaminated air. Therefore, in an urban area or in the vicinity of large point sources, b is approximately equal to b_{scat}.[25]

To estimate a quantitative relationship between light scattering and aerosols, it is necessary to understand the effects of:

- particle size distribution
- aerosol mass concentration
- chemical composition of the aerosol
- particle shape
- relative humidity

Covert et al.[26] discusses the relative importance of each of these variables. Light is scattered most efficiently by particles in the 0.1 to 1.0 μm size range. The premise that scattering efficiency is related to particle mass concentration assumes that the atmospheric particle size distribution is constant. Studies conducted by several researchers tend to support this assumption (Junge,[27] Hidy,[28] Clark and Witby[29]). Such support is important, since the effect of particle size dominates other aerosol properties in determining the extinction coefficient due to light scattering. If the size distribution is fixed and all other factors are constant, the scattering coefficient will be proportional to the mass concentration, i.e.,

$$\frac{M}{b} = \text{constant} \qquad \text{(B6-2)}$$

where M is the aerosol mass concentration. This important relationship, postulated by Charlson et al.,[30] allows one to estimate the distance from which an object on the horizon can be seen (Charlson et al.[30] assigned a factor of two as the level of error for this expression.) However, the equation does little to tell one about degradation in the clarity of objects at given distances from an observer as a function of integrated mass concentration along the line of sight. That is, an actual observer will probably notice a decrease in visual air quality before an object totally disappears from view.

Henry[31] has applied the linear system theory of visual acuity to visibility reduction by aerosols. His approach is based on the assumption that the eye-brain system is nearly linear in its response to light stimulus, and that all objects can be defined in terms of

Fourier combinations of sinusoidal light patterns given in cycles per angular degree of arc. Figure B6-1 illustrates this concept for a spatial frequency of five cycles per degree. This approach leads to the result that, as the integrated mass concentration increases, the smallest discernible sinusoidal frequency of an object decreases, i.e., the visual detail of the object is obscured.

The visual range (V_R) of an object with sinusoidal frequency Q is given by the expression:

$$V_R(Q) = b^{-1} \log \left[\frac{1}{D} \left(\frac{C_M(0)}{C_T(Q)} - 1 \right) + 1 \right] \qquad \text{(B6-3)}$$

where

- b is the extinction coefficient defined in Equation (B6-2);
- $C_M(0)$ is the actual modulation contrast of an object with frequency Q at zero distance, i.e., no degradation due to aerosols, with a representative value of 1, for white or black;
- $C_T(Q)$ is the threshold contrast for frequency Q; and
- D defines the conditions of atmospheric illumination and solar angle (D=1 for full sunlight and D=8 for shadow).

According to Henry,[32] the human eye-brain system is capable of distinguishing object sizes that correspond to a spatial frequency (Q) of 40 to 50 cycles/degree. Objects with frequencies of approximately 30 cycles per degree represent fine detail (e.g., the limb of a tree), a frequency of 15 cycles per degree represents moderate detail (the trunk of a tree) and 5 cycles per degree corresponds to coarse detail (the tree itself). Alternately, visual ranges corresponding to these frequencies represent no reduction in visibility, moderate reduction, and severe reduction.

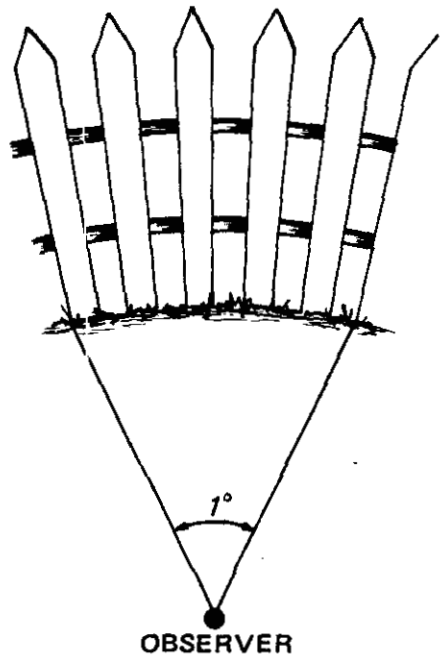

Figure B6-1 Idealized Example Illustrating Spatial Frequency of Five Cycles Per Degree

The Equation (B6-3) can be used to compute visible ranges corresponding to any frequencies for a given aerosol mass concentration as follows. The scattering coefficient b is calculated from Equation (B6-2) with the constant M/b set at 4.5×10^5 $\mu g/m^2$ [30]. Figure B6-2, taken from Henry,[31] illustrates the relationship between the spatial frequency Q and contrast sensitivity ($1/C_T$). Values of contrast sensitivity for 30, 15, and 5 cycles per degree are 4.5, 40, and 250, respectively. In his paper, Henry suggests values of $C_M(0)$ and D=1 for average daylight. For this condition, visible ranges corresponding to frequencies of interest may be calculated from (B6-3). This method was used to assess the effects of emissions from the Hat Creek Project on local visibility.

Ambient relative humidity has an important effect on visibility. Hygroscopic and deliquescent particles in the atmosphere increase in size with increasing humidity. Covert et al.[26] examined light-scattering properties of various atmospheric aerosols for relative humidities ranging from 20 to 100%. In all cases, a dramatic increase in scattering efficiency was noted for relative humidity values greater than 70%. Thuiller et al.[23] also found that for the same aerosol mass distributions, visual range dropped from 12 km for a relative humidity of less than 40% to 6 km when the relative humidity exceeded 40%. They concluded that visual range is not necessarily indicative of aerosol mass concentration for the latter condition.

This dependence of visual range on humidity is important in the case of Hat Creek. On-site relative humidity data indicate that during the winter months (December through February), visible ranges calculated by Equation B6-3 may overestimate the range more than 70% of the time (see Appendix E). Based on results reported by Thuiller et al.,[23] the actual visual range may be only 50% of the computed values during periods of high humidity.

Regional visibility effects and plume opacity were estimated by less formal methods, based on published accounts in the literature and experience at other coal-fired power plants with similar particulate control equipment.

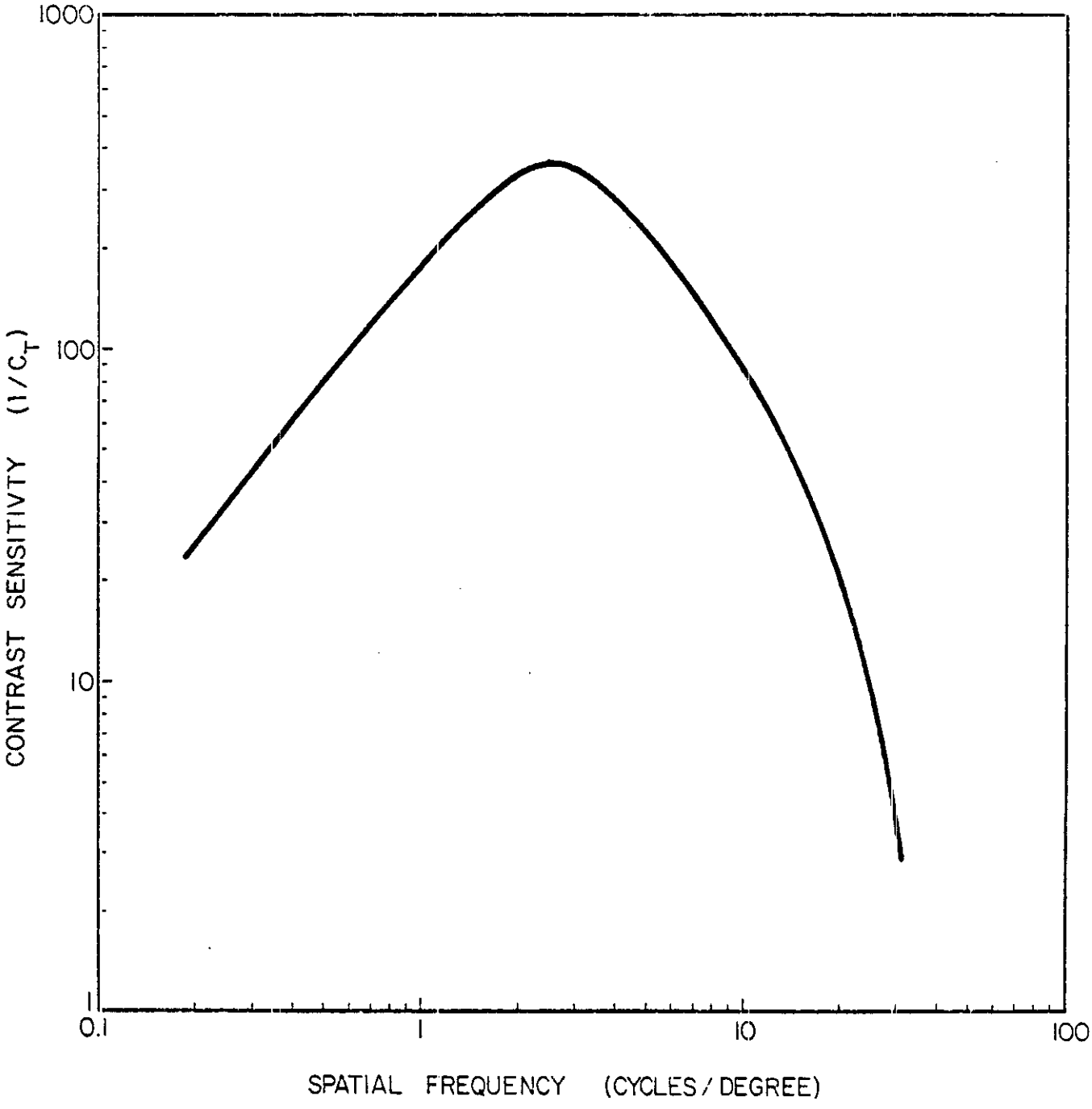

Figure B6-2 Contrast Sensitivity to Sinusoidal Test Patterns

B6.2 ACID PRECIPITATION

Current interest in the relationship between atmospheric contaminants from industrial emissions and acidity in precipitation results primarily from numerous published reports of systematic increases in acidity (decreases in pH) in the waterways of Scandinavia[33,34] and eastern North America.[35,36] In attempting to formulate quantitative predictions of the importance of Hat Creek emissions for changes in precipitation acidity, two major limitations must be recognized:

1) most experimental evidence of acid precipitation has been developed in locations that are frequently downwind of very large industrial regions, hundreds or thousands of square kilometers in size, and with large densities of sulfur and/or nitrogen oxide emissions; and

2) published reports of acid precipitation are based on measurements; some attempts have been made to simulate sulfate deposition by precipitation fallout in Scandinavia, but no modeling techniques to estimate pH change due to a point source were found in the literature.

Obviously the experience in northern Europe and the eastern sections of Canada and the United States cannot be applied directly to British Columbia. Many authors have presented evidence of the relationship between acid rain in Sweden and Norway to long-range transport of plumes from western Europe and the United Kimgdom.[37,28] Similarly, low pH values in the northeastern United States are attributed to emissions in the heavily industrialized Midwest.[39] Thus, locations where acid rain problems exist are generally downwind of high-emission areas extending over hundreds or thousands of square kilometers. This is not the case in the interior of British Columbia. As reported by Summers and Whelpdale,[40] Pacific air masses moving across the province are quite free of anthropogenic contaminants, and even sulfates associated with chlorides from sea spray are largely removed by the time the air reaches the interior of the Province. In fact, evidence is cited by these authors that, except during passage over the Alberta gas fields, eastward-moving air masses remain 'clean' until they reach industrialized southern Ontario.

Widespread pH reduction in rain or snow due to emissions from a power plant is unlikely, since the horizontal area beneath a single plume is small in comparison with that of most storms. Moisture falling through the plume, however, may be measurably affected. The major smelter near Sudbury, Ontario is believed to be responsible for the acidification of nearby lakes and resulting losses among fish populations.[41] However this facility is the world's largest emitter of SO_2, with an emission rate approximately 20 times that of the Hat Creek Plant. Precipitation acidification due to the power plant is expected to be localized and restricted to a relatively narrow area beneath the plume. Meteorological conditions that favor development of a wide, meandering plume are light and variable winds associated with a stagnating high pressure system. Such conditions are unlikely to produce precipitation in any form.

The acidity of precipitation reaching the earth's surface after it has passed through an elevated plume is the result of a series of chemical and physical events that occur before and during precipitation. Sulfur in fossil fuels is oxidized in the combustion process to form SO_2. The SO_2 in the stack gas undergoes further oxidation in the atmosphere to form SO_3^- and $SO_4^=$. The oxidation can occur in a clean environment by photo-oxidation or in the presence of heavy metal catalysts or water. The rate of SO_2 to $SO_4^=$ conversion depends on time of day and the presence or absence of catalytic material. In aqueous solution SO_2 and $SO_4^=$ form sulfuric and sulfurous acids. Nitrogen oxide released by high temperature combustion undergoes similar processes (the reactions are more numerous and complex than for sulfur) to form nitric acid in solution. Acidity in precipitation in the eastern United States and Scandinavia is apparently caused primarily by sulfuric and nitric acids. Less than 15% of the acidity in samples collected at a station in New Hampshire was attributable to organic acids.[42]

The efficiency of precipitation scavenging is important in terms of the amount of acid absorbed by falling moisture. Rain is apparently more efficient than snow in this regard, especially in strong convective situations. The initial pH of the precipitation is also a factor determining the amount of SO_2 dissolved in falling droplets. Dissociation of SO_2 in water to form HSO_3^- and H^+ adheres to conventional laws of chemical equilibrium. Thus, the lower the pH of the precipitation, the lower the solubility of SO_2. Hales et al.[43] concluded that SO_2 absorption would proceed most readily in a rural environment with significant ambient SO_2 concentrations near the surface.

If the vertical distribution of SO_2 concentration is not fairly uniform, SO_2 absorbed by droplets within the plume will be lost to some extent by desorption back to the atmosphere below plume level. It is anticipated that near the Hat Creek site, precipitation passing through the elevated power plant plume will reach the surface with less sulfur than was originally washed out at higher levels. In the following paragraphs, the experience of researchers investigating precipitation chemistry near large power plants is used to estimate acid precipitation effects due to Hat Creek.

Hutcheson and Hall[44] analyzed the results of a precipitation sampling program in the vicinity of a coal-fired power plant in Alabama. They found that sulfate aerosol scavenging alone could not account for observed patterns of washout and suggested that SO_2 scavenging was the primary mechanism. This finding is in contrast to the results of Hales et al.[43] who reported that SO_2 scavenging was less important than sulfate scavenging in explaining observed washout near a large coal-fired plant in Pennsylvania. Hutcheson and Hall[44] explain this apparent contradiction in terms of background concentrations and stack height differences of the two sites. It is postulated that SO_2 scavenging dominates when background concentrations are low, since the 'clean' rain can readily absorb SO_2 as it falls through the plume. If the plume is from a relatively low stack, the reverse desorption process

has less time and less uncontaminated air below the plume in which to proceed. In the Pennsylvania study, the precipitation was presumably acidic before passing through the plume and had more time to desorb below it; consequently, net SO_2 scavenging was relatively unimportant.

The Hat Creek Plant will have a tall stack and will be located in an area with low background contaminant levels. It is anticipated that both SO_2 and $SO_4^=$ scavenging will contribute to wet deposition of sulfates (and acid) near the project site. Experience at other power plants and chemical analysis of snow samples in the interior of the Province indicate that the area below the plume will receive precipitation with pH levels between 4.0 and 5.0 within 20 km during convective summer shower periods. This may be compared with an observed background pH of 5.0 to 5.5 in snow samples taken in the interior of British Columbia (see Appendix A). Note that the area over which these effects will occur will generally be small compared to the total area affected by such storms. In addition, about 42% of the precipitation falling in the Hat Creek Valley is snow. Nyborg and Crepin[45] imply that snow is only about one-fourth as effective in scavenging efficiency as rain.

Potential regional precipitation acidification was estimated on the basis of results of chemical analyses of snow in British Columbia and predicted ambient levels from the diffusion modeling analysis. The maximum predicted hourly sulfate concentration was 0.5 $\mu g/m^3$. The corresponding SO_2 concentration was 1.5 $\mu g/m^3$. These concentrations were assumed to be uniform through a depth of 1500m. The volume of precipitation falling in an area of 1 sq m was determined by the assumed rainfall rate. Different scavenging efficiencies from the literature were postulated to estimate the amounts of SO_2 and $SO_4^=$ absorbed by the falling drops. Results of the snow sample analyses (see Appendix A) were used to calculate the minimum pH corresponding to formation of sulfuric acid in the rainwater by the formula

$$pH = -\log_{10} [10^{A} + \sigma I] \qquad \text{(B6-4)}$$

where

A is the pH without plume washout;

σ is the scavenging efficiency, i.e., percent absorption of SO_2 and $SO_4^{=}$; and

I is the incremental sulfuric acid [equivalents/liter].

An example of the use of Equation (B6-4) follows.

A snow sample collected in early June 1977 in Wells Gray Provincial Park was found to have a pH of 5.1 and an alkalinity of 1.2 mg/liter. The latter number represents the amount of acid that must be added to the solution to reach a pH of 4.5. Expressed in terms of meq/liter, the alkalinity is 0.024. Model results showed an ambient SO_2 concentration of 1.5 $\mu g/m^3$ and a sulfate concentration of 0.5 $\mu g/m^3$ in the vicinity of the park. If <u>total</u> absorption of these species in the precipitation occurs with <u>complete</u> conversion to sulfuric acid and <u>complete</u> dissociation of the acid occurs in the solution, then the total meq of acid added to the sample by washout is 0.0448. Since 0.024 meq are required to bring the pH to 4.5, then the resulting pH is calculated as

$$pH = -\log_{10} [10^{-4.5} + 10^{-3} (0.0448 - 0.024)] = 4.28$$

Considering the conservatism of the assumptions regarding absorption efficiency and dissociation, it is unlikely that the ambient concentrations of SO_x assumed in the above example would ever actually decrease the pH of precipitation to this extent.

Overrein[46] reported that deposition of excess acid in Norway occurs during a few limited periods of rainfall. A station in the southern part of that country received 25% of the excess sulfate in 15 days over a 3-year sampling period. Precipitation acidity in Norway

is associated primarily with long range transport of plumes from western Europe and the United Kingdom. If acid rain from these large area sources occurs only in episodic intervals, it is reasonable to expect that such effects due to a single stack source will occur even more intermittently. Thus, the estimated pH reductions attributable to Hat Creek will occur only occasionally on a regional basis.

B6.3 PHOTOCHEMICAL OXIDANTS

Ozone (O_3) is a highly reactive, colorless gas, formed by the reaction of molecular and ground state oxygen (O_2 and O, respectively). Although O_3 occurs in highest concentrations in the lower stratosphere, the so-called ozonosphere, high levels (greater than 0.10 ppm) are commonly found in polluted areas of the lower troposphere. Due to its effects on human health, vegetation, and materials (especially rubber), O_3 has become a contaminant of widespread concern to scientific and medical researchers as well as regulatory agencies. The production of O_3 in the lower atmosphere occurs mainly by the reactions:

$$NO_2 + h\nu \rightarrow NO + O \qquad \text{(B6-5)}$$

and

$$O + O_2 + M \rightarrow O_3 + M \qquad \text{(B6-6)}$$

where

- $h\nu$ is the ultraviolet light photon for wavelengths less than about 4200Å, and
- M is the catalyst, usually N_2, necessary to dissipate the excess energy produced in the reaction so that the nascent O_3 does not dissociate back to the reactants.

The major mechanism for O_3 loss is reaction with NO:

$$NO + O_3 \rightarrow NO_2 + O_2 \qquad \text{(B6-7)}$$

Ozone formation and destruction in the atmosphere is largely governed by the ratio of NO_2 to NO and by incoming solar radiation; a high NO_2 to NO ratio causes the reaction (B6-5) to dominate, leading to O_3 production, while a low ratio allows NO to deplete O_3 by reaction (B6-7). Since the reaction (B6-1) proceeds at a rate proportional to sunlight intensity, O_3 is formed only during daylight hours. Maximum concentrations normally occur during the period from midday to late afternoon, depending on location of the emissions and from May through September, when sunlight intensity is sufficiently high to produce ozone at latitudes north of 40°.

Changes in the NO_2 to NO ratio can result from reactions involving a variety of atmospheric compounds. For example, hydrocarbon radicals (R), readily oxidize NO through the reaction:

$$RO_2 + NO \rightarrow RO + NO_2 \qquad \text{(B6-8)}$$

which serves to <u>increase</u> the ratio, as does the chain reaction involving CO:

$$\begin{aligned} OH + CO &\rightarrow CO_2 + H \\ H + O_2 &\xrightarrow{M} HO_2 \\ HO_2 + NO &\rightarrow OH + NO_2 \end{aligned} \qquad \text{(B6-9)}$$

and the 3-step reaction involving SO_2:

$$\begin{aligned} SO_2 + OH &\rightarrow HSO_3 \\ HSO_3 + O_2 + M &\rightarrow HSO_5 + M \\ HSO_5 + NO &\rightarrow HSO_4 + NO_2 \end{aligned} \qquad \text{(B6-10)}$$

The HSO_4 can, of course, produce sulfuric acid (which may be converted to sulfate) by abstraction of a hydrogen atom from hydrocarbons or radicals such as HO_2.

Examples of reactions that decrease the NO_2 to NO ratio are:

$$OH + NO_2 \rightarrow HNO_3 \quad \text{(B6-11)}$$

$$HONO + h\nu \rightarrow OH + NO \quad \text{(B6-12)}$$

and

$$NO_2 + NO_3 \rightarrow N_2O_5 \quad \text{(B6- 13)}$$

$$N_2O_5 + H_2O \rightarrow 2HNO_3$$

Emissions from coal-fired power plants are composed primarily of NO, SO_2, and particulates. Radical hydrocarbons, CO, and NO_2 are discharged in much smaller quantities. Near the point of emission, the NO_2 to NO ratio is small and O_3 concentration is low due to reaction (B6-3). Furthermore, reaction (B6-4) is unimportant unless abundant background hydrocarbons are present. Along the plume trajectory, NO is slowly converted to NO_2, largely by reaction with background O_3. As the NO_2 to NO ratio increases, formation of O_3 above background levels can occur far downwind of the source. According to Davis et al.,[47] O_3 concentrations within the plume are lower than ambient levels for many kilometers; Hegg et al.[48] and Ogren et al.[49] describe similar behavior in plumes.

Of the three measurement studies cited, only Davis et al. reported a net increase of plume O_3 above ambient background levels. According to Hegg et al.[48], diffusion within the plume occurs more rapidly than the $NO \rightarrow NO_2$ conversion (and therefore O_3 formation). Net O_3 formation is possible only in areas with high ambient levels of radical precursors, e.g., hydrocarbons, which oxidize NO without involving the background O_3. The Davis[47] study was, in fact, conducted in the Baltimore-Washington D.C. area, an urban locale with relatively high background contaminant concentrations. In a more recent study of the plume from the Labadie power plant near St. Louis, an area of relatively high background hydrocarbons, Gillani et al.[50] also observed a net increase of O_3 far downwind (e.g., 190 km) from the plant. The findings of Ogren et al.[49] and Hegg et al.[48] correspond to measurements in areas with low background levels, and may be considered more representative

of applicability to the Hat Creek Project. This site is located in a region where reactive hydrocarbon concentrations are expected to be very low (probably less than 1.0 ppb). In view of the probable lack of precursors necessary for formation of excess O_3, it is concluded that the Hat Creek Plant plume will not be a source of significant O_3 above existing ambient levels.

B6.4 NITROGEN OXIDES

Atmospheric oxidation of NO emitted from a coal-fired power plant involves a complicated series of reactions that depend on background concentrations of many contaminants, including hydrocarbons, hydroxyl and hydroperoxyl radicals, as well as other stack plume constitutents. Due to the complicated nature of the processes governing the transformation of NO to NO_2 and organic and inorganic nitrates, it is necessary to rely on experimental results of other studies to estimate the potential effects of Hat Creek NO_x emissions.

Based on their work at the 1200 Mw Centralia power plant in Washington, Hegg et al.[48] determined that the time required to convert 50% of the plume NO to NO_2 is roughly proportional to the square of plume travel time. Although one might expect a steadily increasing NO_2 to NO ratio with increased travel distance, these researchers found that the conversion process is diffusion-controlled. It is, therefore, more likely that the ratio will have an upper limit that depends on meteorological conditions and the background O_3 concentration (see Section B6.3).

The maximum NO_2 to NO ratio observed at Centralia was 4.3. This value is probably near the upper limit for the prevailing conditions at Centralia, since the ratio increases only very slowly with time after the first ten minutes.

The HCM used to calculate local and regional NO_x concentrations due to Hat Creek emissions does not simulate the complex chemistry of NO oxidation to form NO_2 and organic and inorganic nitrates. As indicated by the foregoing discussion, any attempt to do so would necessarily involve a series of speculative assumptions regarding background levels of numerous air quality parameters. Rather, to estimate incremental NO and NO_2 concentrations, the conversion of NO was taken into account by adjusting the NO and NO_2 emission rates to reflect probable conversion rates. On the basis of the Centralia results, an initial NO_x emission of 50% NO and 50% NO_2 (by volume) was assumed for the local modeling (maximum downwind distance of 25 km). For the regional modeling applications, it was assumed that 80% of the NO_x emissions were in the form of NO_2.

Elevated nitrate levels are commonly observed in areas downwind of large NO_x emission sources, since NO and NO_2 are precursors to the formation of both organic and inorganic nitrates. Nitric acid (HNO_3) is the most common species of inorganic nitrate formed in the atmosphere. The reactions most frequently associated with HNO_3 production are:

$$OH + NO_2 + M \rightarrow HNO_3 + M \qquad \text{(B6-14)}$$

$$N_2O_5 + H_2O \rightarrow 2HNO_3 \qquad \text{(B6-15)}$$

In the atmosphere, nitric acid formed by such reactions exists as nitrate salts, since HNO_3 reacts with many other compounds. For example, gaseous ammonia reacts with nitric acid to form NH_4NO_3, ammonium nitrate.

The organic nitrates are formed chiefly by reactions with hydrocarbon radicals, e.g.,

$$RO + NO_2 \rightarrow RONO_2 \qquad \text{(B6-16)}$$

Peroxyacetyl nitrate (PAN) results from the reaction:

$$RCO_3 + NO_2 \rightarrow RCO_3NO_2 \qquad \text{(B6-17)}$$

Organic nitrates can reach significant levels in polluted areas, e.g., PAN concentrations of 50 ppb (parts per billion) are recorded in the Los Angeles Basin. However, the lack of substantial hydrocarbon sources to produce radical precursors in the Hat Creek region should limit the production of these compounds to very low ambient levels (<1 ppb).

B7.0 REFERENCES

1. Austin, J. M. 1975. Massachusetts Institute of Technology. Unpublished Notes.

2. Weisman, B. and M. S. Hirt 1975. Meteorological Assessment of the Hat Creek Valley. Part I. MEP Company.

3. Weisman, B. and M. S. Hirt 1975. Meteorological Assessment of the Hat Creek Valley, Study II, Part 1. MEP Company.

4. Hovind, E. L., T. Spangler, and N. Graham 1977. Summary of Results of Plume Simulation Studies in the Hat Creek Valley. North American Weather Consultants. Goleta, California.

5. U.S. Nuclear Regulatory Commission 1972. On-site Meteorological Programs. Regulatory Guide 1.23.

6. Eschenroeder, A. 1975. An Assessment of Models for Predicting Air Quality. ERT Document 75-03. Santa Barbara, California.

7. Roth, P. M., M. A. Yocke, J. P. Meyer, M. Liu, and J. P. Killus 1975. An Examination of the Accuracy and Adequacy of Air Quality Models and Monitoring Data for Use in Assessing the Impact of EPA Significant Deterioration Regulations on Energy Developments. Report prepared for Greenfield, Attaway, and Tyler, Inc., San Rafael, California.

8. Briggs, G. A. 1969. Plume Rise. U.S. AES Critical Review Series. Oak Ridge, Tennessee.

9. Smith, M. 1951. The Forecasting of Micrometeorological Variables. Meteorological Monographs 1. No. 4. American Meteorological Society.

10. American Society of Mechanical Engineers (ASME) 1968. Recommended Guide for the Prediction of Dispersion of Airborne Effluents. New York, New York.

11. Briggs, G. S. 1976. Personal Communication.

12. Bosanquet, C. H., W. F. Caregy, and E. M. Halton 1950. Proceedings of the Institute of Mechanical Engineers, 62, p. 355. London.

13. Egan, B. A. 1975. Turbulent Diffusion in Complex Terrain. AMS Workshop on Air Pollution Meteorology and Environmental Assessment. Boston, Massachusetts.

14. Queney, P., G. A. Corby, N. Gerbier, H. Koschnieder, and J. Zierup 1960. The Air Flow Over Mountains. World Meteorological Organization. Technical Report No. 34. (ed. M.A. Alaka) p. 135.

15. Wilson, R. B., G. E. Start, C. R. Dickson, and N. R. Ricks 1976. Diffusion under Low Wind Speed Conditions near Oak Ridge, Tennessee. Doc. NOAA. Technical Memo ERL ARL-61.

16. Lague, J. 1973. Observed Entrainment in a Power Plant Plume. M.S. Thesis. Massachusetts Institute of Technology.

17. Hidy, G. M., E. Y. Tong and P. K. Mueller 1976. Design of the Sulfate Regional Experiment (SURE). Vol. 1. Electric Power Research Institute. EL-125, Palo Alto, California.

18. Houghton, H. G. and W. H. Radford 1938. On Measurement of Drop Size and Liquid Water Content in Fogs and Clouds. Pop. Phys. Ocean. Meteor. MIT. Woods Hole Oceanogr. Inst. No. 4.

19. Slawson, P. R., J. H. Coleman, and J. W. Frey 1974. Some Observations of Cooling Tower Plume Behavior at the Pardise Steam Plant. Tennessee Valley Authority. Muscle Shoals, Alabama.

20. Meyer, J. H., I. W. Eagles, L. C. Kohlenstein, J. A. Kagan, and W. D. Stanbro 1974. Mechanical Draft Cooling Tower Visible Plume Behavior: Measurements, Models, Predictions. Presented at Cooling Tower Environment 1974. March 4-6. University of Maryland. College Park, Maryland.

21. Overkamp, T. J. and D. P. Hoult 1971. Precipitation in the Wake of Cooling Towers. Atmospheric Environment. Vol. 5. Pergamon Press. Oxford, England. 14 pp.

22. Hanna, S. R. 1974. Meteorological Effects of the Mechanical Draft Cooling Towers of the Oak Ridge Gaseous Diffusion Plant. Atmospheric Turbulence and Diffusion Laboratory. Contribution No. 89. Oak Ridge, Tennessee. 23 pp.

23. Thiuller, R., J. Sandber, W. Siu, and M. Feldstein 1973. Suspended Particulate and Relative Humidity as Related to Visibility Reduction. No. 73-138. Presented at the 66th Annual Meeting of the Air Pollution Control Association.

24. Koschmieder, H. 1924. Beitr. Phys. Freien Atm. Vol. 12 pp. 33-53, 171-181.

25. Charlson, R. J. 1969. Atmospheric Visibility Related to Aerosol Mass Concentration. Environmental Science and Technology. Vol. 3. No. 3. pp. 913-918.

26. Covert, D. S., R. J. Charlson, and N. C. Ahlquist 1972. A Study of the Relationship of Chemical Composition and Humidity to Light Scattering by Aerosol. Journal of Applied Meteorology. Vol. II. pp. 968-976.

27. Junge, C. E. 1952. Ber. Deut. Wetterd. Vol. 35. pp. 261-277.

28. Hidy, G. M. 1965. Journal of Colloid Science. Vol. 20. pp. 123-144.

29. Clark, W. E. and K. T. Whitby 1967. Journal of Atmospheric Science. Vol. 24. pp. 677-687.

30. Charlson, R. J., N. C. Ahlquist and H. Hovarth 1968. On the Generality of Correlation of Atmospheric Aerosol Mass Concentration and Light Scatter. Atmospheric Environment. Vol. 2. pp. 455-464.

31. Henry, R. C. 1977. The Application of the Linear System Theory of Visual Acuity to Visibility Reduction by Aerosols. Atmospheric Environment. Vol. 11. pp. 697-701.

32. Henry, R. C. 1978. Personal Communication.

33. Oden, S. 1975. The Acidity Problem--An Outline of Concepts. Proceedings of the First International Symposium on Acid Precipitation and the Forest Ecosystem. L. S. Dochinger and T. A. Seliga ed. U.S.D.A. Forest Service General Technical Report NE-23 pp. 1-36.

34. Landsberg, H. 1954. Some Observations of the pH of Precipitation Elements. Archiv für Meteorologie. Geophysik und Bioklimatologie Serie A: Meteorologie Geophysik. Vol. 7.

35. Likens, G. E. and F. H. Bormann 1974. Acid Rain: A Serious Regional Environmental Problem. Science. 184:1176-1179.

36. Beamish, R. J. and H. H. Harvey 1974. Loss of Fish Populations from Unexploited Remote Lakes in Ontario, Canada as a Consequence of Atmospheric Fallout of Acid. Water Research 8:85-95.

37. Nord Ø, J. 1976. Long Range Transport of Air Pollutants in Europe and Acid Precipitation in Norway. pp. 87-103. In: Dochinger, L. S. and T. A. Seliga, ed. Proceedings of the First International Symposium on Acid Precipitation and the Forest Ecosystem, U.S.D.A. Forest Service General Technical Report NE-23. 1074p.

38. Reed, L. E. 1976. The Long-Range Transport of Air Pollutants. Ambio. 5(5,6):202.

39. Coghill, C. and G. Likens 1974. Acid Precipitation in the Northeastern United States. Water Resources Research 19A: 1133-1137.

40. Summers, P. W. and D. M. Whelpdale 1976. Acid Precipitation in Canada. pp. 411-421. In: Dochinger, L. S. and T. A. Seliga, ed. Proceedings of the First International Symposium on Acid Precipitation and the Forest Ecosystem. U.S.D.A. Forest Service General Technical Report NE-23. 1074p.

41. Beamish, R. J. 1976. Acidification of Lakes in Canada by Acid Precipitation and the Resulting Effect on Fishes. pp. 479-498. In: Dochinger, L. S. and T. A. Seliga, ec. Proceedings of the First International Symposium on Acid Precipitation and the Forest Ecosystem. U.S.D.A. Forest Service General Technical Report NE-23. 1074p.

42. Galloway, J. N., G. Likens, and E. Edgerton 1976. Hydrogen Ion Speciation in the Acid Precipitation of the Northeastern United States. pp. 383-396. In: Dochinger, L. S. and T. A. Seliga, ed. Proceedings of the First International Symposium on Acid Precipitation and the Forest Ecosystem, U.S.D.A. Forest Service General Technical Report NE-23. 1074p.

43. Hales, J. M., J. M. Thorpe, and M. A. Wolf 1971. Field Investigation of Sulfur Dioxide Washout from the Plume of a Large Coal-Fired Power Plant by Natural Precipitation. Environmental Protection Agency. Air Pollution Control Office Contract No. CPA-22-69-150.

44. Hutcheson, M. R. and F. P. Hall, Jr. 1974. Sulfate Washout from a Coal Fired Power Plant Plume. Atmospheric Environment. Vol. 8, pp. 23-28.

45. Nyborg, M. and J. Crepin 1976. Effect of Sulphur Dioxide on Precipitation and on the Sulphur Content and Acidity of Soils in Alberta, Canada. pp. 767-777. In: Dochinger, L. S. and T. A. Seliga, ed. Proceedings of the First International Symposium on Acid Precipitation and the Forest Ecosystem. U.S.D.A. Forest Service General Technical Report NE-23. 1074p.

46. Overrein, L. N. 1976. Impact of Acid Precipitation on Forest and Freshwater Ecosystems in Norway. Summary Report on the Research Results from the Phase I (1972-1975) of the SNSF Project. Oslo.

47. Davis, D., G. Smith, and G. Klaubert 1974. Trace Gas Analysis of Power Plant Plumes via Aircraft Measurements: Ozone, NO_x, and SO_2 Chemistry. Science. 186. pp. 733-736.

48. Hegg, D. A., P. Hobbs, and L. F. Radke 1976. Reactions of Nitrogen Oxides, Ozone, and Sulfur in Power Plant Plumes. EPRI Report EA270.

49. Ogren, J. A., D. L. Blumenthal, and W. H. White and Systems Applications Inc. 1976. Determination of the Feasibility of Ozone Formation in Power Plant Plumes. EPRI Report EA307.

50. Gillani, M. V., R. B. Husar, J. D. Husar, D. E. Patterson, and W. E. Wilson, Jr. 1977. Project MISTT: Kinetics of Particulate Sulfur Formation in a Power Plant Plume Out to 300 Km. Paper presented at the International Symposium on Sulfur in the Atmosphere. September 7-14. Dubrovnik, Yugoslavia.

ADDENDUM A

(A)1.0 THE HAT CREEK MODEL

(A)1.1 FORMULATION AND ASSUMPTIONS

The Hat Creek Model (HCM) calculates ground level contaminant concentrations due to emissions from the proposed power plant stack. The basic equation of the model is the Gaussian plume expression relating ambient concentrations to emissions in terms of a meteorological function (e.g., see Turner[1]). Specifically,

$$X(x,y,z) = \frac{Q(o,o,H)}{2\pi\sigma_y\sigma_z U} \exp\left[-1/2\left(\frac{y}{\sigma y}\right)^2\right] \cdot \left[\exp\left[-1/2\left(\frac{z-H}{\sigma_z}\right)^2\right] + \exp\left[-1/2\left(\frac{z+H}{\sigma_z}\right)^2\right]\right] \quad \text{(A-1)}$$

where

- (x,y,z) are the coordinates (along-wind, crosswind, and vertical) of a Cartesian system with origin at the emission source (O,O,H) [length].
- $X(x,y,z)$ is the ground-level contaminant concentration at receptor location (x,y,z) [mass/length^3]. In the present applications, ground-level centerline concentrations (corresponding to y=o in Equation A-1) were calculated for each hour.
- Q is the source emission rate [mass/time].
- H is the effective height of emission (stack height plus plume rise) and, thus, the elevation of the plume centerline above the ground [length].
- σ_y, σ_z are dispersion coefficients indicating plume spread rate in the cross-wind and vertical directions, respectively [length].
- U is the average wind speed at stack height [length/time].

The most important model assumptions are the following:

1) Wind speed and direction are uniform throughout the field of receptors (points at which concentrations are computed) during the period corresponding to each application of Equation A-1. However, wind speed is assumed to vary with height above the ground.

2) Emission rate is constant and the meteorological parameters governing plume behavior are unchanged over the basic calculation period throughout the field of receptors.

3) The plume leaving the stack rises until it reaches an equilibrium elevation; the height of the plume centerline is corrected to reflect lifting over terrain obstacles.

4) At any downwind distance, the maximum concentration is found at the plume centerline. The profiles of contaminant mass in the cross-wind and vertical dimensions are well described by Gaussian (normal) distributions.

5) Concentration profiles of concentration described by the Gaussian formulation are not instantaneous distributions; rather, they represent average plume spread over an hour. Consequently, they incorporate the variability of wind flow and turbulence associated with this time period.

6) All contaminant mass is conserved, i.e., none of the emitted material is lost due to chemical transformations, deposition, or washout by precipitation. (In the adaptation of the model for regional applications this assumption is modified. See Section A1.5.)

Assumptions 1) and 2) are characteristics of a steady-state model representation. Assumption 6) is valid for modeling contaminant transport and dispersion on a local scale. Removal processes do not significantly deplete the plume from a tall stack for a period of several hours. For this reason, different assumptions are necessary to simulate local and regional behavior. In the present study, 'local' is understood to refer to radial distances of 25 km or less from the source.

A1.2 DISPERSION COEFFICIENTS

The spread of contaminants released to the atmosphere is governed by turbulent eddy motions. The characteristic size of the eddies at a given time and location determines the rate at which an airborne plume will be diluted by entrainment of outside air. The degree of such mixing permitted by ambient conditions is generally referred to as atmospheric stability. Stability is related to the vertical profile of temperature, the wind speed, solar insolation, and the nature of the underlying ground surface. Unstable conditions favor rapid dilution of plume material; stable conditions characteristically suppress mixing.

The HCM incorporates the assumption that horizontal and vertical profiles of concentration in a contaminant plume resemble Gaussian (or normal) distributions. Thus for a given stability, a measure of dispersion at a particular distance from a plume source is provided by the standard deviations, σ_y and σ_z, of these distributions. Functional forms describing the along-wind variation of these so-called dispersion coefficients for different stabilities have been suggested for point source applications by many investigators, e.g., Pasquill[2], Gifford[3], and Turner[1]. The applicability of various dispersion coefficients depends largely on the experimental conditions under which they were derived.

The horizontal and vertical dispersion coefficients used in the HCM closely resemble those developed at Brookhaven National Laboratory and published by the American Society of Mechanical Engineers[4]. However, the specific expressions used for σ_y and σ_z stem from a model calibration analysis based on gas tracer plume simulation experiments conducted in the Hat Creek Valley. A comprehensive description of the calibration methods and resulting dispersion coefficients is presented in Addendum C of this Appendix.

Some explanation of the dispersion assumptions for multiple-hour average concentrations is warranted. The coefficients developed from the gas tracer studies are taken to represent an averaging period of one hour. The hourly concentrations calculated by means of Equation A-1 are ground-level centerline values, i.e., the maximum concentration at the downwind distances corresponding

to model receptor locations. For times greater than three hours, simple averaging of these maxima is considered unduly conservative, since the wind direction is specified in the model only in terms of the appropriate 22.5° sector. Thus, for longer averaging times, the hourly centerline concentrations are modified by a factor that effectively replaces the centerline value by a value corresponding to uniform distribution of the plume across the wind direction sector. Multiple-hour average concentrations for all periods greater than three hours are then formed by taking the arithmetic mean of these 'sector-averaged' one-hour values. This approach was also adopted in computing three-hour averages for periods characterized by very light winds (less than 2 mps) accompanied by stable conditions. In these circumstances, natural variability of wind direction at a given elevation, and pronounced directional shear in the vertical tend to spread plume material in the cross-wind sense, so that three-hour averages formed from hourly centerline concentrations are considered overly conservative.

(A)1.3 PLUME RISE

The HCM uses the most recent plume rise equations of Briggs[5]. For unstable and neutral conditions:

$$\Delta h = \frac{1.6F^{1/3} x^{2/3}}{u} \qquad (x < 3.5\ x^*) \qquad \text{(A-2)}$$

$$\Delta h = \frac{1.6F^{1/3}(3.5\ x^*)^{2/3}}{u} \qquad (x \geq 3.5\ x^*) \qquad \text{(A-3)}$$

where

F is the buoyancy flux of stack emissions (m^4/sec^3)

x^* is the downwind distance at which atmospheric turbulence dominates entrainment in plume rise (m)

x^* is $14\ F^{5/8}$ if $F \leq 55\ m^4/s^3$ (A-4)

x^* is $34.49\ F^{2/5}$ if $F > 55\ m^4/s^3$ (A-5)

$3.5\ x^*$ is the downwind distance at which the plume becomes level (m)

For stable conditions:

$$\Delta h = \frac{1.6\ F^{1/3}\ x^{2/3}}{u} \qquad (x < 2.4\ u\ s^{1/2}) \qquad \text{(A-6)}$$

$$\Delta h = 2.9 \left(\frac{F}{us}\right)^{1/3} \qquad (x \geq 2.4\ u\ s^{1/2}) \qquad \text{(A-7)}$$

where

$$F = \frac{g\ V_e r_s^2\ (T_s - T_a)}{T_s} \qquad \text{(A-8)}$$

s is the stability parameter based on atmospheric lapse rate

$$s = \frac{\partial\theta}{\partial z}\ \frac{g}{T_a} \qquad \text{(A-9)}$$

and

$\partial\theta/\partial z$ is the rate of change of potential temperature with height (°K/m)

g is the acceleration due to gravity (9.81 m/sec^2)

T_a is the ambient temperature (°K)

V_e is the exit velocity of the stack gas (m/sec)

r_s is the stack radius (m)

T_s is the exit temperature of stack gas, (°K)

u is the wind speed at h_s (m/sec)

The equation for plume rise in a calm atmosphere, defined by winds less than 1.4 m/sec, is as follows:

$$\Delta h = 5.0\ F^{1/4}\ s^{-3/8} \qquad \text{(A-10)}$$

The wind speed, u, at stack height h_s, was computed from the value measured at 10m above the ground by a power-law expression:

$$U(h_s) = U_{10m} \left(\frac{h_s}{10}\right)^p \qquad \text{(A-11)}$$

where the exponent p has values of 0.09, 0.14, and 0.20 for unstable, neutral, and stable conditions respectively.

(A)1.4 PLUME TRAPPING

Equation A-1 is used to predict short-term concentrations for the condition of unlimited mixing. Vertical dispersion can be substantially affected by the presence of an elevated inversion having a base above the effective height of emission. Such an inversion base acts as a 'lid' to restrict vertical eddy motions, and dispersion of contaminants trapped within the underlying atmosphere layer is not well described by Equation A-1.

Following the suggestion of Turner,[1] a modified expression is used to compute ground-level concentrations for restricted mixing conditions. If the computed plume rise exceeds the mixing height, it is assumed that the plume will not disperse downward through the inversion layer, and the effect upon concentrations at downwind receptors at ground level is negligible. When the effective stack height is below the mixing height, concentrations are calculated as follows. Equation A-1 is used for distances less than X_T, defined as the downwind distance at which σ_z = 0.47D (D is the mixing depth). Beyond a distance $2X_T$. uniform vertical mixing between the ground and the mixing height is assumed. For distances between X_T and $2X_T$, vertical diffusion is treated by interpolation between the extremes for unlimited and complete mixing. Specifically, the basic dispersion equation can be rewritten more generally as:

$$X(x,y,z) = \frac{Q}{U} \text{ vdf . hdf} \qquad \text{(A-12)}$$

where

vdf is a vertical dispersion function, and

hdf is a horizontal dispersion function.

Note that for unlimited mixing or for downwind distance X less than X_T, ground-level centerline concentrations are computed with

$$vdf = \frac{1}{\sqrt{2\pi}\sigma_z}\left[\exp\left[-\frac{1}{2}\left(\frac{z-H}{\sigma_z}\right)^2\right] + \exp\left[-\frac{1}{2}\left(\frac{z+H}{\sigma_z}\right)^2\right]\right] \qquad \text{(A-13)}$$

as in Equation A-1. For limited dispersion caused by an elevated inversion, concentrations are computed between X_T and $2X_T$ by the multiple-reflection expression proposed by Turner[1] (Equation 5.8, page 36). Beyond the distance $2X_T$, uniform mixing between the inversion base and the ground is assumed.

(A)1.5 THE EFFECTS OF TERRAIN

The HCM incorporates procedures to adjust the height of a plume to account for the presence of terrain features in the vicinity of the Hat Creek Project. Model inputs include elevations corresponding to each receptor point. For neutral and unstable conditions, the plume centerline is assumed to be lifted by an amount equal to one-half the rise of the terrain above the stack base elevation. Figure (A)-1 illustrates this 'half-height correction' in the HCM. For stable stratification, it is assumed that the plume centerline passes closer to the ground surface; the terrain correction factor for this case is 0.1, and the plume is assumed to pass around the side of a hill, rather than over it. For neutral stability, the half-height correction to the Gaussian plume equation results in predicted concentrations consistent with those expected from potential flow theory for plumes passing over an idealized spherical obstruction (Egan[6]). Queney et al.[7] have demonstrated that a plume is lifted with an equivalent terrain correction factor of 0.2 to 0.4 during stable flow over an infinitely long ridge. The existing evidence indicates a plume should pass more closely to three-dimensional than to two-dimensional features by about a factor of two. For example, the approach distance to an isolated peak would be about half that expected over a long ridge. The 10% correction used in HCM for stable conditions is considered a reasonable (yet conservative) simulation estimate.

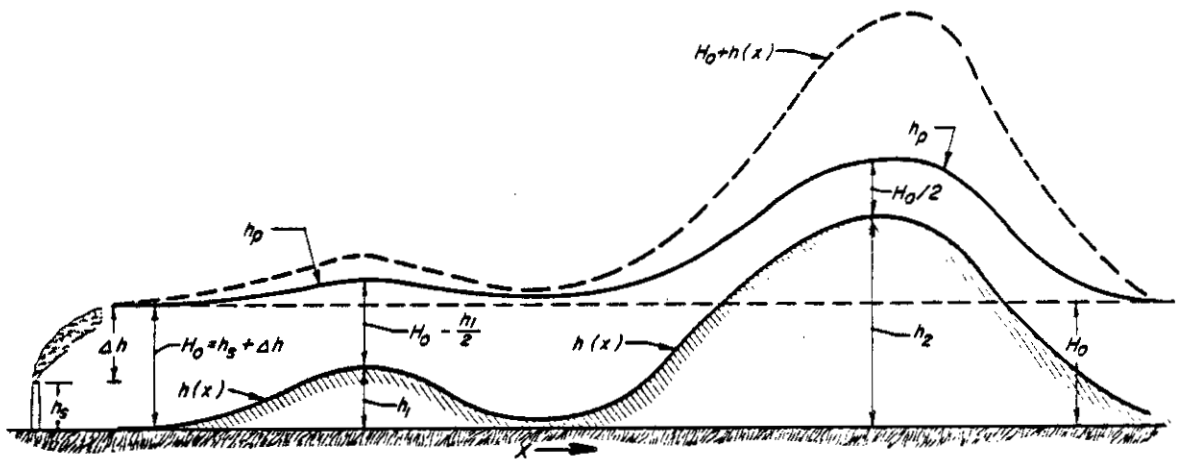

h_s is physical stack height
Δh is plume rise
H_0 is effective stack height (physical stack height plus plume rise)
h(x) is terrain height above stack base elevation
h_p is plume centerline height above stack base elevation

Figure (A)-1 Terrain Height Correction in the Hat Creek Model

B00202

(A)1.6 THE HAT CREEK REGIONAL MODEL

The model used to compute air quality effects of the proposed power plant on a regional scale, i.e., for radial distances of 25 to 100 km from the site, is similar in formulation and assumptions to the HCM previously described. Indeed, most of the material regarding the HCM presented thus far in this Addendum is also applicable in the context of analysis methods used for the regional modeling. Consequently, only differences between the HCM and its regional version are discussed in this section. The principal differences in terms of applications in this study are:

- meteorological input
- treatment of chemical reaction processes
- treatment of contaminant deposition.

(a) Meteorological Input

Whereas the HCM uses meteorological input data in the form of a sequence of hourly values, the regional model was operated with weather data in the form of a stability wind rose developed from 700 mb observations at Vernon, B.C. This wind rose is presented in Appendix A. Thus, applications of the regional model are confined to calculation of long-term, e.g., season or annual average, contaminant concentrations.

(b) Chemical Reaction Processes

The regional model incorporates consideration of simple atmospheric reactions, whereby a plume contaminant is gradually transformed into a secondary species. In particular, the depletion of plume SO_2 to form $SO_4^=$ is accounted for in the regional modeling for the Hat Creek air quality assessment. The loss of a primary contaminant species is calculated by means of the relationship

$$\chi_1 = \chi_o \exp\left(\frac{-\lambda X}{U}\right) \qquad \text{(A-14)}$$

where

X_o is primary species concentration in the absence of chemical decay loss

X_1 is primary species concentration after chemical decay loss

λ is reaction rate constant

X is downwind distance

U is mean wind speed

Secondary contaminants are formed from the loss of primary contaminant material.

A value of 4.16×10^{-6} sec^{-1} (1.5% per hour) was assumed for the rate of conversion (λ) from SO_2 to $SO_4^=$. This value compares favorably with published rates, e.g., Hidy[8], Eliassen and Saltbones[9], and Lusis and Weibe[10].

Oxidation of NO in the atmosphere is an extremely complex process governed by many processes including photooxidation, oxidation in the presence of particulate catalysts, and reactions with hydrocarbons. Consequently, the formation of NO_2 in the plume cannot be simulated by a simple expression such as Equation (A-14). According to Hegg et al.,[11] NO to NO_2 conversion in a power plant plume is diffusion-limited. The maximum NO_2/NO ratio found by the authors in the plume of the Centralia power plant in Washington was 4.3. It may be assumed that this ratio represents a near-maximum value, since the ratio grows very slowly after about ten minutes.

Because of the complexity of the atmospheric conversion processes, the decay of NO and formation of NO_2 are simulated indirectly by means of adjusted stack emission rates. For the local-scale modeling, emission rates for NO and NO_2 were calculated on the premise that the volume of NO_x in the stack gas is equally apportioned as NO and NO_2. For regional-scale applications, the results of Hegg et al.[11] were incorporated, i.e., NO_2 was assumed to account for 80% of the volume of NO_x leaving the stack.

(c) Contaminant Deposition

The regional model was used to compute average dry deposition rates as well as ambient concentrations of plume contaminant species. For a given species the deposition rate is found by the relationship

$$M = \chi \cdot UV_d$$

where

- M is the mass deposition rate [mass/length^2/time]
- χ is the ground-level ambient concentration [mass/length^3]
- U is the mean wind speed [length/time], and
- V_d is the characteristic deposition velocity divided by a nominal wind speed [dimensionless]

Values of the deposition velocities used for SO_2, $SO_4^=$, NO, NO_2, and TSP in the regional model applications are:

- SO_2: 1.0 cm/sec (Reference 9)
- $SO_4^=$: 0.1 cm/sec (Reference 9)
- NO, NO_2: 0.1 cm/sec (Reference 12)*
- TSP: assumed same as $SO_4^=$ value for regional transport

In the regional model, depletion of, e.g., plume SO_2 and $SO_4^=$ by deposition is not accounted for in the calculation of ambient SO_2 and $SO_4^=$ further downwind. Thus plume concentrations of both species are probably overestimated.

*Authors of Reference 12 actually reported a deposition velocity for NO_x of 0.5 cm/sec for experimental work in the Los Angeles area. This value is considered excessive for Hat Creek modeling. A 0.1 cm/sec deposition velocity is assumed for both NO and NO_2.

(A)2.0 REFERENCES

1. Turner, D. B. 1969. Workbook of Atmospheric Dispersion Estimates. U.S. Dept. HEW. Public Health Service. NAPCA. Cincinnati.

2. Pasquill, F. 1961. The estimation of the Dispersion of Windborne Material. Meteorol. Mag. 90: 1063. pp. 33-49.

3. Gifford, F. A. 1961. Uses of Routine Meteorological Observations for Estimating Atmospheric Dispersion. Nuclear Safety. 2: 4. pp. 47-51.

4. ASME 1968. Recommended Guide for the Prediction of Dispersion of Airborne Effluents. M. Smith (ed). New York, NY.

5. Briggs, G. A. 1970. Some Recent Analyses of Plume Rise Observations. Second International Clean Air Congress of the International Union of Air Pollution Prevention Association. Washington, D.C.

6. Egan, B. A. 1975. Turbulent Diffusion in Complex Terrain. American Meteorological Society Workshop on Meteorology and Environmental Assessment. Boston, MA.

7. Quency, P., G. A. Corby, N. Gerbier, H. Koschnieder, and J. Zierup 1960. The Air Flow Over Mountains. World Meteorological Organization. Technical Report No. 34. (ed. M.A. Alaka) p. 135.

8. Hidy et al. 1976. Design of the Sulfate Regional Experiment (SURE). Electric Power Research Institute, Report EC-21. Palo Alto, CA.

9. Eliassen, A. and J. Saltbones 1975. Decay and Transformation Rates of SO_2 as Estimated from Emission Data, Trajectories, and Measured Air Concentrations. Atmospheric Environment 9: pp. 425-429.

10. Lusis, M. A. and H. A. Weibe 1976. The Rate of Oxidation of Sulfur Dioxide in the Plume of a Nickel Smelter. Atmospheric Environment 10: pp. 793-798.

11. Hegg, D. A., P. Hobbs, and L. Radke 1976. Reactions of Nitrogen Oxides, Ozone and Sulfur in Power Plant Plumes. Electric Power Research Institute. Report EA-270. Palo Alto, CA.

12. Jerskey, T. N. et al. 1976. Sources of Ozone: An Examination and Assessment. Report No. EF76-HOR prepared for American Petroleum Institute by Systems Applications, Inc.

ADDENDUM B

(B)1.0 ERT AIR QUALITY MODEL (ERTAQ)

(B)1.1 FORMULATION AND ASSUMPTIONS

ERTAQ was used to estimate short-term and annual concentrations of TSP resulting from fugitive dust emissions in the proposed Hat Creek coal mine. ERTAQ is a Gaussian model similar to the HCM described in Addendum A. However, the ERTAQ formulation is designed for applications involving multiple sources, including point, line, and area sources. These capabilities are necessary for estimating air quality effects due to the various dust-producing activities of the mine.

ERTAQ incorporates most of the same basic assumptions as the HCM in that: (1) steady-state conditions are simulated; (2) horizontal and vertical profiles of emitted material from an individual source are assumed to conform to Gaussian profiles; and (3) plume contaminant mass is conserved. In addition, the dispersion coefficients are the same as those described in Addendum A, Section (A)1.2.

Since dust from the mine results from emissions at or near the ground, without excess buoyancy or velocity, no plume rise calculations are included in the concentration calculations. Instead, emissions are assumed to be mixed uniformly through an initial 10-m depth.

The air quality effects of the mine are considered to be limited to the Hat Creek Valley, and TSP concentrations are calculated to a maximum distance of 10 km. Depletions or transformations of plume material due to chemical reactions or deposition are not considered in the ERTAQ formulation.

Wind speed is assumed constant with height and throughout the field of model receptors for each hourly period. Trapping by elevated inversions and plume penetration of such inversions are not considered for surface mining applications. The ERTAQ model does not incorporate methods for plume height correction due to terrain effects.

Both short-term (24-hour) and annual average concentrations were calculated with appropriate meteorological data.

(B)1.2 METEOROLOGICAL INPUT DATA

Annual average TSP concentrations due to fugitive dust emissions from the proposed mine were calculated by ERTAQ with an annual stability wind rose developed from hourly data collected during 1975 at the B.C. Hydro Mechanical Weather Station No. 5, near the mine site. Tabulations of the stability wind rose are presented in Appendix A.

Short-term concentrations were also calculated for comparison with 24-hour ambient guidelines. For these simulations, separate sets of meteorological input parameters were chosen to represent a range of potential worst-case dispersion conditions. These conditions were identified from the stability wind rose and from wind persistence statistics developed for mechanical weather stations in the valley. Light-wind/stable (stagnation) as well as high-wind/neutral situations were investigated. In addition to these extremes, several other weather scenarios were modeled to obtain realistic estimates of more typical air quality conditions in the Hat Creek Valley.

(B)1.3 AREA SOURCES AND LINE SOURCES

The ERTAQ model computes ambient concentrations resulting from any combination of multiple point, line, and area sources. With the few exceptions noted in Section (B)1.1, the ERTAQ treatment for point sources is similar to that in the HCM (see Addendum A). The emissions from trucks dumping coal at transfer points are examples of mining activities modeled as point sources.

Area sources include the major pit operations (shoveling, blasting, and scraping). To simulate air quality effects due to a rectangular area source $Q_A(x,y,H)$, the equation for the concentration at a given receptor located at grid point (0,0,Z) is:

$$\chi(0,0,\ ) = \int_{x_1}^{x_2} d_x \int_{y_1}^{y_2} d_y \frac{Q_a(x,y,H)}{\sqrt{2\pi}\ \sigma_z\ U} \qquad \text{(B-1)}$$

$$\cdot\ hdf(x,y) \left\{ \exp\left[-\frac{1}{2}\left(\frac{z-H}{\sigma_z}\right)^2 \right] + \exp\left[-\frac{1}{2}\left(\frac{z+H}{\sigma_z}\right)^2 \right] \right\}$$

where

x_1, x_2 are projections of the area source on an axis parallel to the mean wind (see Figure (B)-1) [length]

y_1, y_2 are projections of the area source on an axis perpendicular to the mean wind

Q_a is emission rate [mass/length^2/time].

H is effective plume height [length]

σ_z is vertical dispersion coefficient [length]

hdf is a horizontal dispersion function; for multiple hour averages, hdf = 1/c where c = 2xtan (11.25°) = 0.398x

Computer realization of Equation B-1 is achieved by dividing each area source into a number of rectangular elements oriented perpendicular to the wind direction. The area source integration then involves the summation of contributions from each elemental area. This technique represents an advancement over most previous methods which simulate contributions of area sources by a series of closely-spaced virtual point sources.

For a uniform, constant line source distribution, the concentration at the point (0,0,z) is the integral along the line of elemental strips of length dl

$$\chi(0,0,z) = \frac{Q}{U} \oint_{x_1,y_1}^{x_2,y_2} V(0,0,z;x,y,H) \qquad \text{(B-2)}$$

with the transfer function V given for time average calculations by

$$V(0,0,z,x,y,H) = hdf(x,y) \cdot Vdf(x,y) \qquad \text{(B-3)}$$

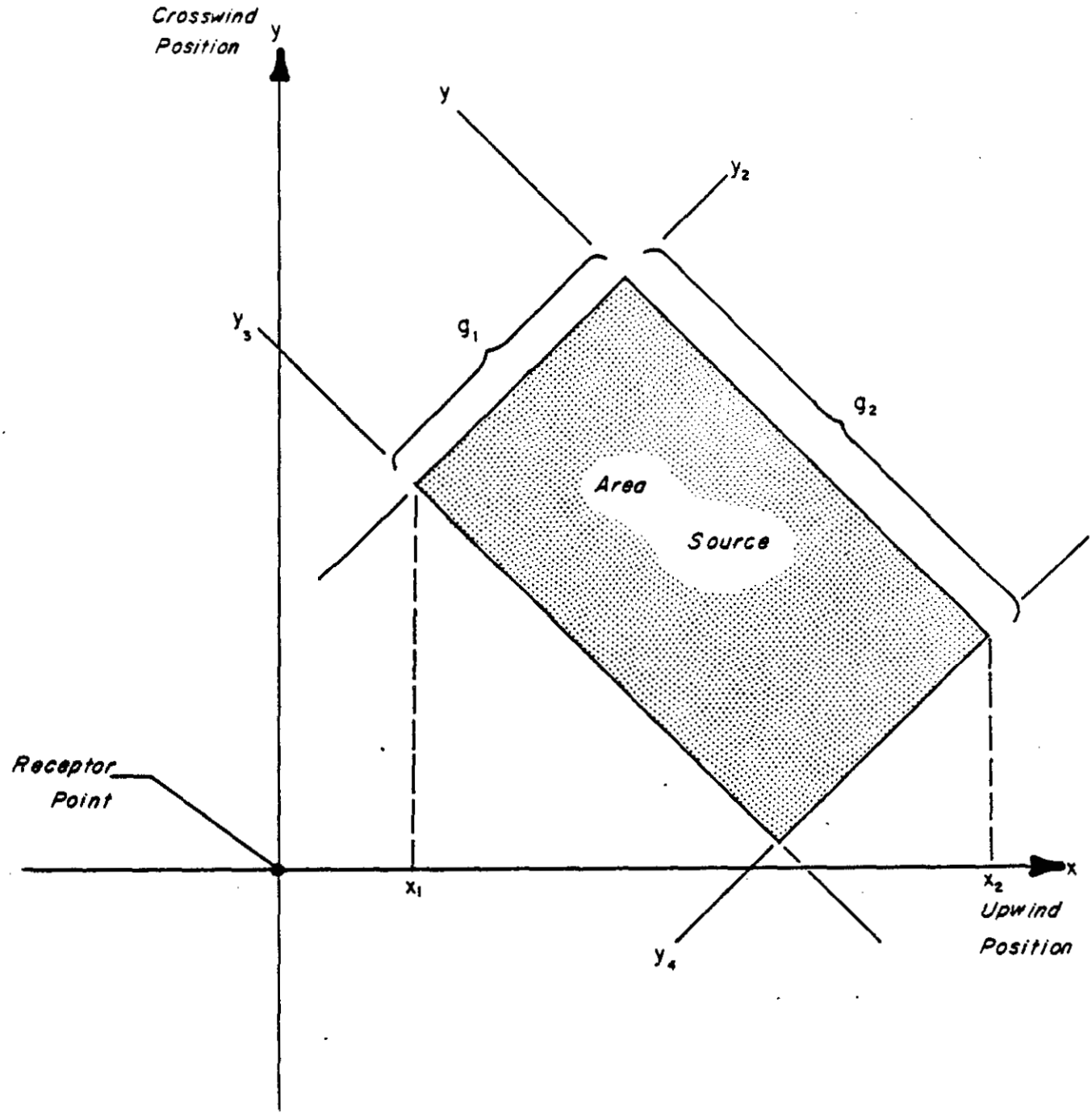

Figure (B)-1 Area Source Representation in the ERTAQ Model

where

$$hdf = \frac{c(x) - y}{c^2(x)} \qquad \text{(B-4)}$$

$c(x) = 0.398\ x = 2x\tan(11.25°)$ = sector width at distance x,

and

$$vdf = \frac{1}{2\pi\sigma_z}\left[\exp\left[-\frac{1}{2}\left(\frac{z-H}{\sigma_z}\right)^2\right] + \exp\left[\frac{1}{2}\left(\frac{z+H}{\sigma_z}\right)^2\right]\right]. \qquad \text{(B-5)}$$

The numerical integration of Equation B-2 is accomplished by representing the line integral as a summation over a set of M virtual points, and displaced upwind by an amount that increases the sector width c by Δy:

$$\chi(0,0,z) = \frac{Q}{U}\,\Delta\ell \sum_{k=1}^{M} V(0,0,z;\ x_k, y_k, H) \qquad \text{(B-6)}$$

The modified sector width $c^1 = 0.398\ x + |\Delta y|$ is then used in Equation B-4.

The geometry corresponding to determination of $\chi(0,0,z)$ due to a line source is illustrated in Figure (B)-2. Examples of line sources associated with the coal mine include vehicle operations over unpaved roads and the maintenance and construction of haul roads.

(B)1.4 ANNUAL AVERAGING SCHEME

Short-term (hourly) concentrations, χ, resulting at a particular receptor as a result of a given source are calculated for each combination of wind speed, wind direction, and stability taken from the stability wind rose. The annual average concentration, $\bar{\chi}$, is obtained by summing over the contribution due to each weather condition weighted by its relative frequency of occurrence during the year. The average concentration is then given by

$$\bar{\chi} = \sum_K \sum_L \sum_J F(J,K,L)\chi(J,K,L) \qquad \text{(B-7)}$$

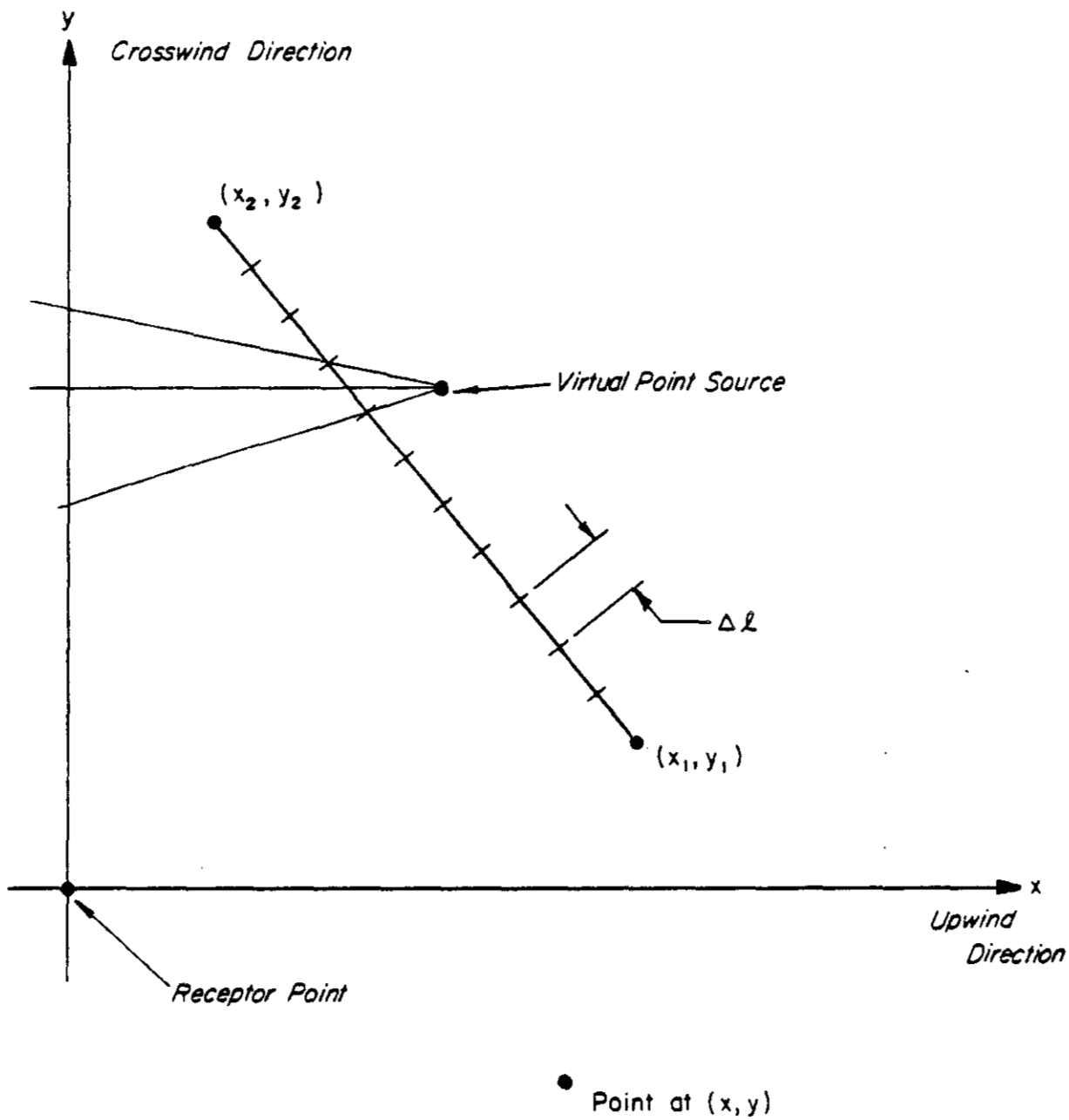

Figure (B)-2 Line Source Representation in the ERTAQ Model

5476

where

$F(J,K,L)$ is the normalized frequency for the combination of wind direction K, wind speed class J, and stability class L.

$\chi(J,K,L)$ is the hourly concentration for the same weather condition.

Annual averages at specific receptors are obtained by summing the results from Equation B-7 over all sources.

ADDENDUM C

(C)1.0 CALIBRATION OF THE HCM

(C)1.1 DATA BASE

To apply a mathematical model to simulate dispersion of airborne contaminants at a given geographic location, it is useful to collect enough meteorological, emissions, and concentration information to calibrate the model. Recognizing this fact, B.C. Hydro contracted with NAWC to conduct a series of gaseous tracer releases. The testing program was conducted in two parts, one during the late winter (February 16-23, 1976 and March 22-26, 1976) and one during the late summer (July 31-August 11) of 1976. The purpose of these test series was to determine the diffusion characteristics of an elevated plume diffused under a variety of temperature and wind fields over the rough terrain of the area.

Oil fog and sulfur hexafluoride (SF_6) were released from an aircraft to simulate emissions from the proposed power plant located within the Hat Creek Valley system. These tracer plumes were tracked by an instrumented aircraft which made passes through the plume at various altitudes and distances from the release point. Among the instruments on board the tracking aircraft was a nephelometer, which measured the degree of light scatter from the oil fog droplets. It was this oil fog backscatter data that was primarily used in the calibration of the dispersion model. Ground level concentrations of SF_6 were also measured during the tracer studies. These added to the data base for calibration.

Pibal and minisonde releases were made during the hours of the plume sampling tests to measure the wind fields and vertical temperature gradients.

ERT received plume transect data from NAWC in the form of nephelometer backscatter concentrations, time, altitude, and horizontal location.

Data from the pibal and minisonde releases (vertical temperature and wind profiles) were for the most part presented in graphical form. The NAWC experiments analyzed by ERT to calibrate the model are summarized in Table (C)-1.

(C)1.2 ERT TECHNICAL APPROACH

To calibrate the Hat Creek and cooling tower models, ERT determined the horizontal and vertical dispersion coefficients (σ_y and σ_z) of the oil fog plume based upon the available backscatter data. Once these coefficients were calculated for the various test meteorological conditions (i.e., lapse rate and wind speed) and distances from the release point, plume diffusion rate based upon these coefficients were extrapolated for other downwind distances by use of a power law $\sigma = ax^b$. The constants 'a' and 'b' were determined by the least squares best fit through the points representing the dispersion coefficients and where x is the downwind distance.

Nephelometer backscatter data were given to ERT in the form of discrete concentrations points along with the corresponding altitude and horizontal locations. For each pass through the plume at a given altitude, an average of 10 concentration data points were given in the horizontal. In order to determine σ_y, the second moment about the plume center of mass was determined. The equations for this technique are as follows:

$$Y_o = \sum\left[Y_i \cdot \chi(Y_i)\right] / \sum\left[\chi(Y_i)\right] \qquad \text{(C-1)}$$

where Y_o is the the center of mass

$\chi(Y_i)$ is the concentration at point Y_i

and

$$\sigma_y^2 = \sum\left[\chi(Y_i) \cdot (Y_i - Y_o)^2\right] / \sum \chi(Y_i) \qquad \text{(C-2)}$$

TABLE (C)-1

NAWC TRACER RELEASE EXPERIMENTAL PARAMETERS

Date	Test	Distance From Release (km)	No. of Passes	Mean Wind Speed (m/sec)	Mean Lapse Rate (°C/100m)	Release Point
2/19/76	1	1.5	10	1.0	+0.18	Lower Site
2/19/76	1	2.5	3	1.0	-0.34	Lower Site
2/20/76	2	3.6	13	6.0	-0.67	Lower Site
2/21/76	3	1.6	12	7.5	-0.28	Upper Site
7/31/76	6	5.2	2	5.0	-0.44	Upper Site
7/31/76	6	8.8	3	5.0	-0.44	Upper Site
7/31/76	6	16.8	4	5.0	-0.52	Upper Site
7/31/76	6	20.0	3	5.0	-0.52	Upper Site
8/1/76	7	2.9	9	2.5	-0.59	Upper Site
8/1/76	7	6.9	5	2.5	-0.51	Upper Site
8/5/76	8	3.4	7	3.5	-0.65	Upper Site
8/5/76	8	7.4	4	3.5	-0.65	Upper Site
8/6/76	9	3.3	13	1.0	-0.96	Lower Site
8/7/76	10	3.0	9	1.5	-0.54	Upper Site
8/9/76	11	4.4	16	8.0	-0.44	Upper Site
8/9/76	11	14.0	7	8.0	-0.44	Upper Site
8/9/76	11	20.4	4	8.0	-0.69	Upper Site
8/10/76	12	2.8	14	2.5	-0.82	Upper Site
8/10/76	12	10.6	14	2.5	-0.84	Upper Site
8/10/76	13	1.5	14	1.5	-0.93	Upper Site
8/11/76	14	4.4	11	3.5	-0.70	Upper Site
8/11/76	14	16.9	7	3.5	-0.69	Upper Site
8/11/76	14	45.3	7	3.5	-0.67	Upper Site

From the theory of a Gaussian distribution, σ_y is independent of the vertical distance from the center of the plume as long as the concentration does not fall below the threshold of the measuring instrument.* Therefore, the σ_y's from all of the passes through the plume over a given geographic location were averaged to determine a mean σ_y for that downwind distance from the point of release.

The oil fog was released by an aircraft flying in a horizontal circular pattern with a diameter of 260m. Therefore, the 'plume' had an initial spread before it diffused and was transported downstream. To adjust for this initial crosswind spread a virtual point source was assumed to be located upwind from the release point. To do this, it was assumed that the initial tracer cloud had a normal distribution and that the visible edge of the cloud marked the point at which the concentration was 10% of the cloud centerline concentration. Based upon this assumption, the σ_y of the cloud was approximately 60m. The tests were conducted during thermally neutral or slightly stable atmospheric conditions. Because the power law constants 'a' and 'b' had not yet been determined, it was necessary to use available horizontal dispersion curves to estimate σ_y of the plume. Thus, the Pasquill-Gifford curves, representative of the appropriate stability, were used to give an estimate of the distance from the release point to the virtual point source. Comparisons with other diffusion parameterization schemes revealed that differences in the calculated value of the distance to the virtual point source were slight and within the limits of error inherent in the experimental approach. On the average, the distance to the assumed virtual point source was approximately 1 km. This correction was made only for σ_y calculations. No correction was required for σ_z since the initial vertical spread was negligible.**

An error analysis (f-test) was performed to determine if the horizontal distribution of concentration measurements conformed to the basic Gaussian assumption. This test was performed by finding the best Gaussian fit through the concentration distribution for each pass through the plume.

*Similarly, σ_z is independent of the crosswind (horizontal) distance.

**It should be noted that a buoyant plume would induce vertical plume growth because of buoyant turbulence. This was not accounted for by the oil fog releases.

If the F-ratio for that distribution showed that a better fit could have been obtained more than 10% of the time by fitting the same curve through a random distribution of concentrations, the corresponding σ_y was not used in calculating the mean σ_y for that downwind distance. Finally, the confidence interval for $\bar{\sigma}_y$ (see error limits of σ_y in Table (C)-2) was determined at the 95% level.

Because it was difficult to determine if the entire plume has been sampled in the vertical, it was necessary to compute σ_z based upon the assumptions that the plume had a normal distribution in the vertical and that the aircraft pass through the plume that recorded the highest concentration was the pass through the geometric center of the plume.* Based upon these two assumptions, σ_z was computed in the following manner.

The crosswind integrated concentration ($\chi_{(cic)}$) for the assumed centerline transect was calculated by numerically integrating the measured concentrations. Because of variations of the vertical temperature structure of the atmosphere during the tracer studies, σ_z was calculated using two variations of the general formula for $\chi_{(cic)}$. For tests when the tracer was released above a temperature inversion, the formula for $\chi_{(cic)}$ that incorporates the effects of a reflecting surface (the inversion top) on the centerline concentration was used to relate the numerically computed $\chi_{(cic)}$ to the theoretical equation based on σ_z. For these cases the formula for $\chi_{(cic)}$ is:

$$\chi_{(cic)} = \left(\frac{2}{\pi}\right)^{1/2} \frac{Q}{\sigma_z \bar{u}} \qquad \text{(C-3)}$$

where $\bar{u}$ is the mean horizontal wind speed (m/sec)

Q is the source strength (g/sec)

*Although it is recognized that this assumption has a small effect on the estimated value of σ_z, missing the highest concentration could cause a slight overestimate of the magnitude of σ_z.

TABLE (C)-2

GAUSSIAN DISPERSION COEFFICIENTS DERIVED FROM NAWC STUDY

Test	Distance (km)	Virtual Distance (km)	σ_y(m)*	σ_z(m)
1	1.5	2.6	654 ± 76	147
1	2.5	3.6	1262 ± 550	93
2	3.6	4.5	287 ± 58	311
3	1.6	2.5	447 ± 94	69
6	5.2	6.3	267 ± 298	128
6	8.8	9.7	208 ± 95	413
6	16.8	17.7	326 ± 150	159
6	20.0	20.9	842**	372
7	2.9	4.0	302 ± 66	112
7	6.9	7.8	303 ± 51	212
8	3.4	4.3	382 ± 65	57+
8	7.4	8.3	380 ± 602	131+
9	3.3	4.2	740 ± 200	434+
10	3.0	3.9	456 ± 23	99+
11	4.4	5.3	270 ± 34	86+
11	14.0	14.9	435 ± 95	114+
11	20.4	21.3	661 ± 464	98+
12	2.8	3.9	269 ± 26	45
12	10.6	11.5	411 ± 77	27+
13	1.5	2.4	783 ± 145	275+
14	4.4	5.3	470 ± 147	70+
14	16.9	17.8	836 ± 306	93+
14	45.3	46.2	536 ± 676	224+

*Confidence level for $\bar{\sigma}_y$ at the 95% level.

**Calculated from one pass through the plume.

+Reflection term not included in calculation.

Seven tests were conducted when the tracer was released above an inversion layer.

There were five tests conducted when no temperature inversions were present. The plume was high enough above the ground in the vicinity of the release for these cases that reflection from the earth's surface did not contribute to the concentrations observed at the plume centerline. The applicable formula for calculating $\chi_{(cic)}$ is:

$$\chi_{(cic)} = \frac{1}{2} \left(\frac{2}{\pi}\right)^{1/2} \cdot \frac{Q}{\sigma_z \bar{u}} \qquad \text{(C-4)}$$

The calculated values of σ_y and σ_z are presented in Table (C)-2.

(C)1.3 DATA ANALYSIS

Once the data received from NAWC were processed to yield the horizontal and vertical diffusion coefficients, an extensive analysis was performed to determine which atmospheric parameters had the greatest effect on the horizontal and vertical diffusion within the plume. The results are summarized in Table (C)-3.

The analysis indicates that σ_y is most strongly influenced by the wind speed as opposed to lapse rate or wind direction as indicated by the correlation coefficients listed in the table. On the other hand, σ_z is mostly influenced by the atmospheric lapse rate. Sagendorf[1] obtained similar results in investigating diffusion under low wind speed conditions. The results of his study indicate that it is most desirable to determine σ_y based upon fluctuations of the horizontal wind while the best approximation of σ_z is obtained using lapse rate.

The following approach was used to determine how the diffusion coefficients correlated with various atmospheric conditions. To investigate the correlation with wind speed, the diffusion coefficients were subdivided into various wind speed categories ($\leq$ 2.0 m/sec, etc). The curve represented by the expression $\sigma = ax^b$, which is the best fit through the data points in a category, was determined. The correlation

TABLE (C)-3

STATISTICAL ANALYSIS OF NAWC PLUME MEASUREMENTS

Sigma Y (σ_y)	Number of Points	R Correlation	F Ratio	Probability of Exceeding F (%)
$\bar{u}^* \leq 2.0$	6	.85	10.93	2.5
$2.0 > \bar{u} \leq 5.0$	14	.77	17.66	.2
$\bar{u} > 5.0$	6	.82	8.05	4.0
$\gamma^+ > -.5$	8	.28	.68	45.0
$-.5 \geq \gamma \geq -.75$	13	.77	16.72	.2
$\gamma < -.75$	5	.59	1.59	30.0
North Wind**	9	.86	20.29	.3
South Wind	15	.33	1.69	20.0
Sigma Z (σ_z)				
$\bar{u} \leq 2.0$	5	.00	.00	100.0
$2.0 > \bar{u} \leq 5.0$	13	.47	3.07	10.0
$\bar{u} > 5.0$	5	.00	.00	100.0
$\gamma > -.5$	9	.50	2.28	15.0
$-.5 \geq \gamma \geq -.75$	12	.37	1.61	20.0
$\gamma < -.75$	4	.66	1.61	40.0
North Wind	8	.32	1.38	25.0
South Wind	14	.20	0.22	80.0

*$\bar{u}$ is the mean horizontal wind speed (m/sec).

**Any wind direction between 270° and 360° or between 00° and 090°.

+γ is the lapse rate of the vertical layer containing the oil fog plume (°C/100 m)..

coefficient (R) and the F ratio were then generated for the best fit curve through the points. If the data exhibited a high degree of correlation (large value of R) and the probability of exceeding the F ratio by a random distribution of points is less than 10%, then it was assumed that σ_y exhibited a high correlation for that wind speed category. Finally, if σ_y satisfied the above criteria for all wind speed categories, it was assumed that σ_y was highly correlated with wind speed. This general procedure was carried out for σ_y and σ_z for wind speed, wind direction, and lapse rate. Figures (C)-1 through (C)-8 depict the results.

(C)1.4 ANALYSIS OF σ_y

Table (C)-3 shows that σ_y exhibits a high correlation with a lapse rate between -0.5°C/100m and -0.75°C/100m. Closer examination, however, reveals 80% of the points within this range of lapse rate also fall in the wind speed category between 2.0 m/sec and 5.0 m/sec (see Table (C)-1 and (C)-2). Therefore, it appears that the correlation in this case may be a manifestation of the correlation with wind speed rather than a correlation with temperature gradient, especially considering the weaker correlations with the other lapse rate categories.

An examination of the graph of σ_y versus distance, where σ_y has been classified according to wind speed (Figure (C)-2) reveals that the lighter wind speed cases ($\bar{u} \leq 2.0$ m/sec) show large values of σ_y as compared to σ_y values for the higher wind speed ($\bar{u} > 2.0$ m/sec). This is consistent with work done by Markee (Yanskey et al.[2]), which indicated that plume meander is enhanced under light wind speed conditions, resulting in larger values of σ_y than anticipated using standard classification schemes. Markee derived a new set of horizontal dispersion curves where the smallest value of σ_y occurred during neutral conditions and the values of σ_y increased with increasing stability under low wind speed conditions. The tracer data available from the Hat Creek Valley indicate that enhanced horizontal diffusion during periods of wind speed less than 2.0 m/sec can be expected in the region.

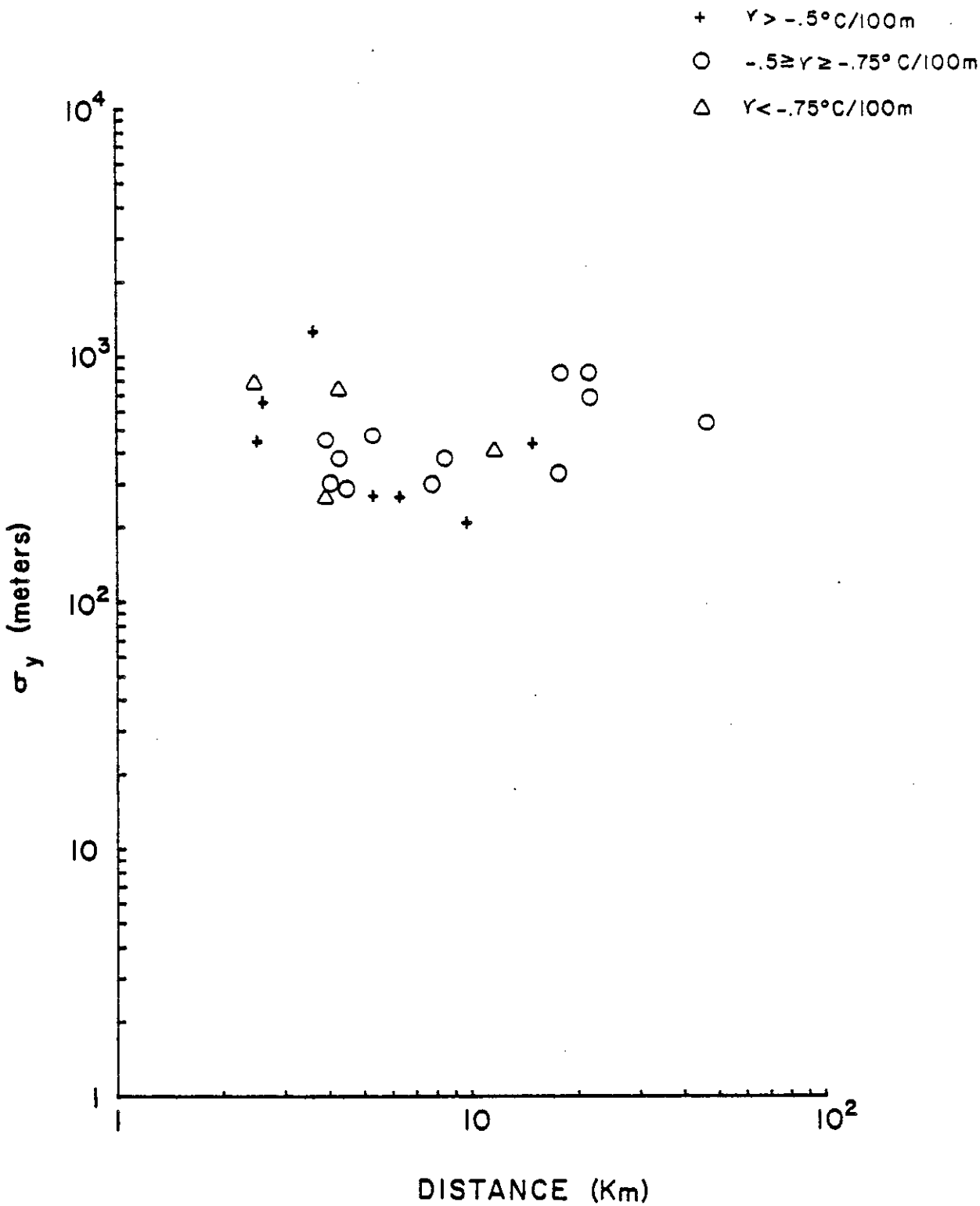

Figure (C)-1 σ_y Classified by Lapse Rate

804318

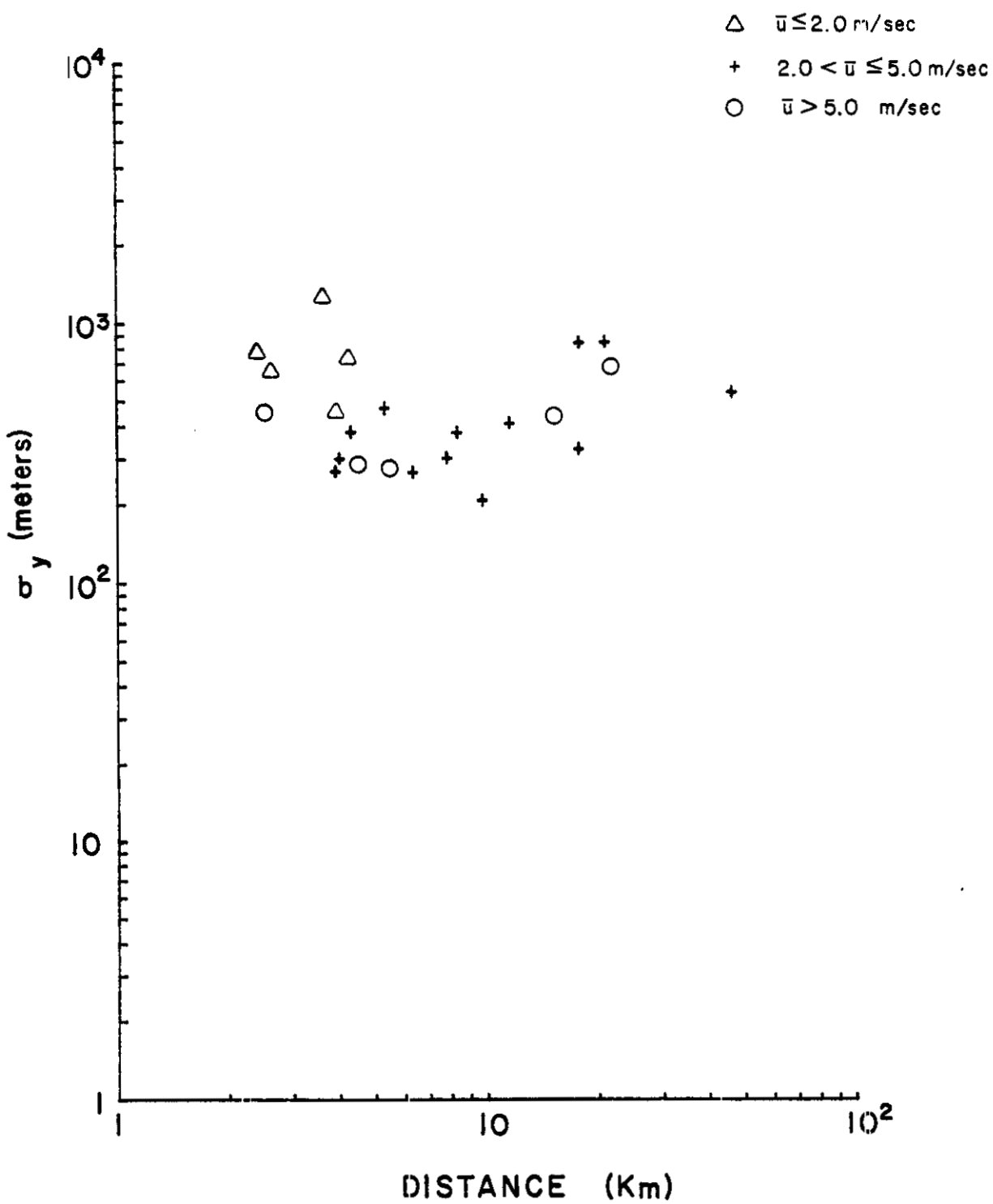

Figure (C)-2 σ_y Classified by Wind Speed

804319

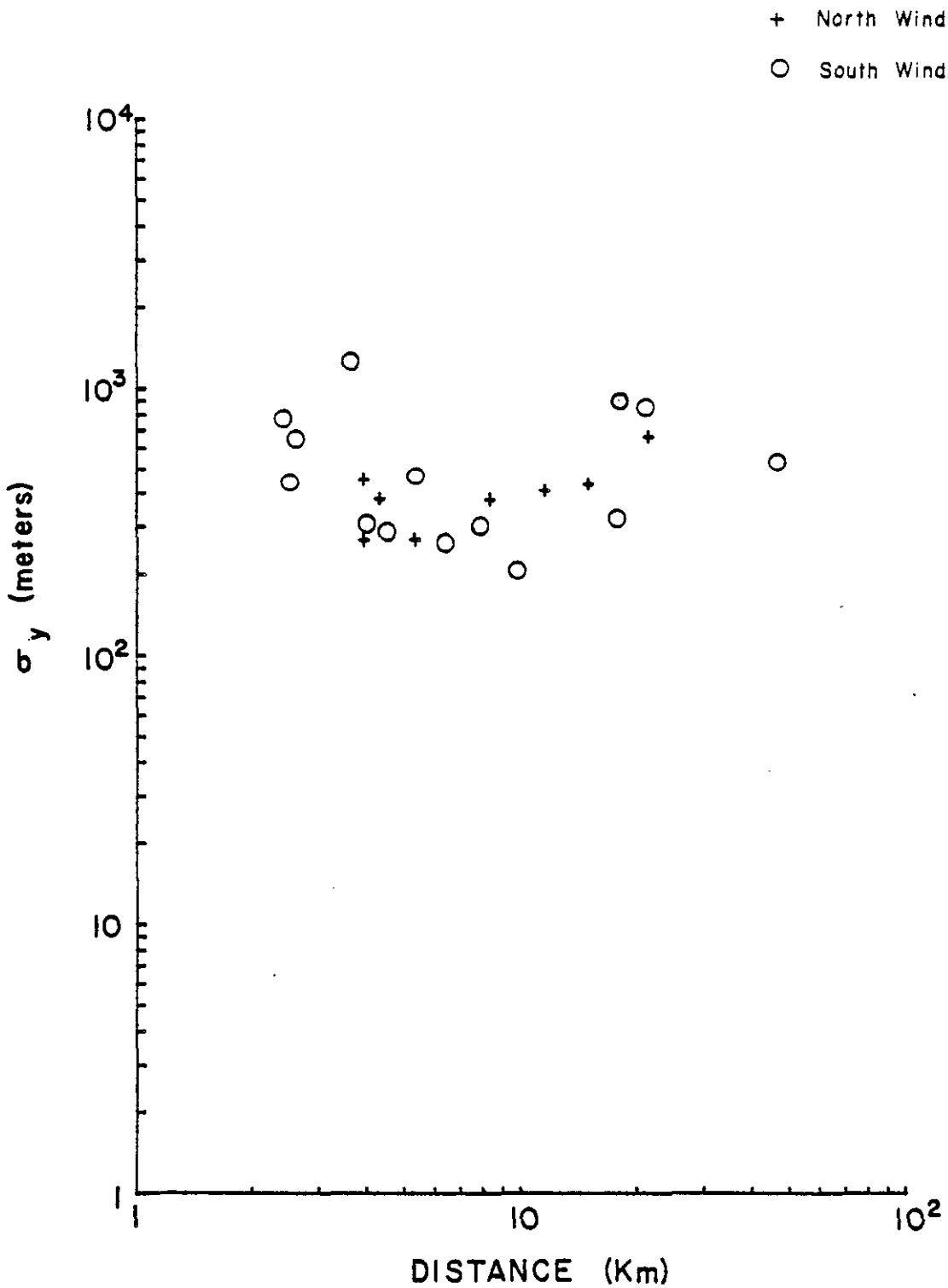

Figure (C)-3 σ_y Classified by Wind Direction

804320

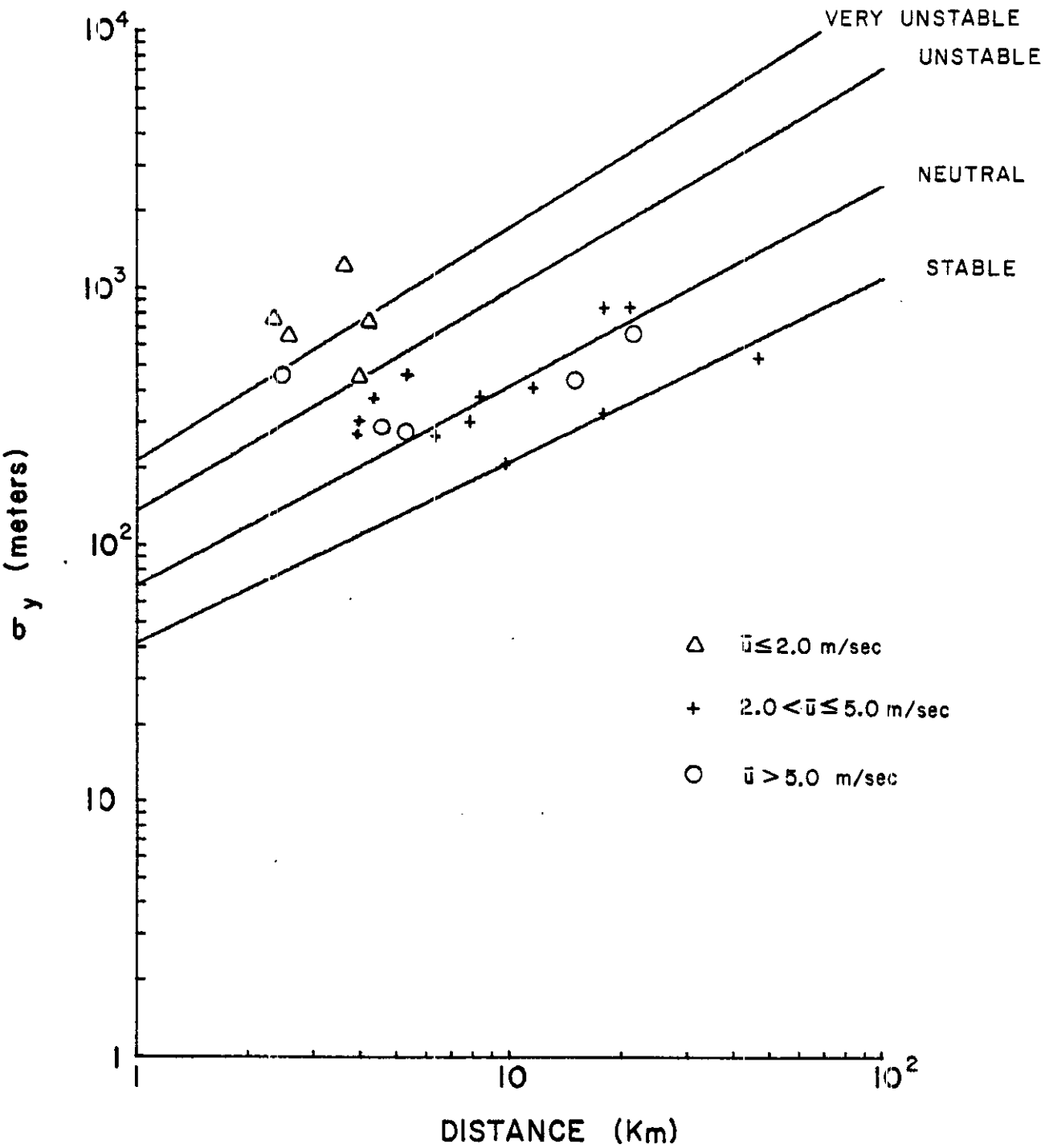

Figure (C)-4 ASME Curves through σ_y Data

804321

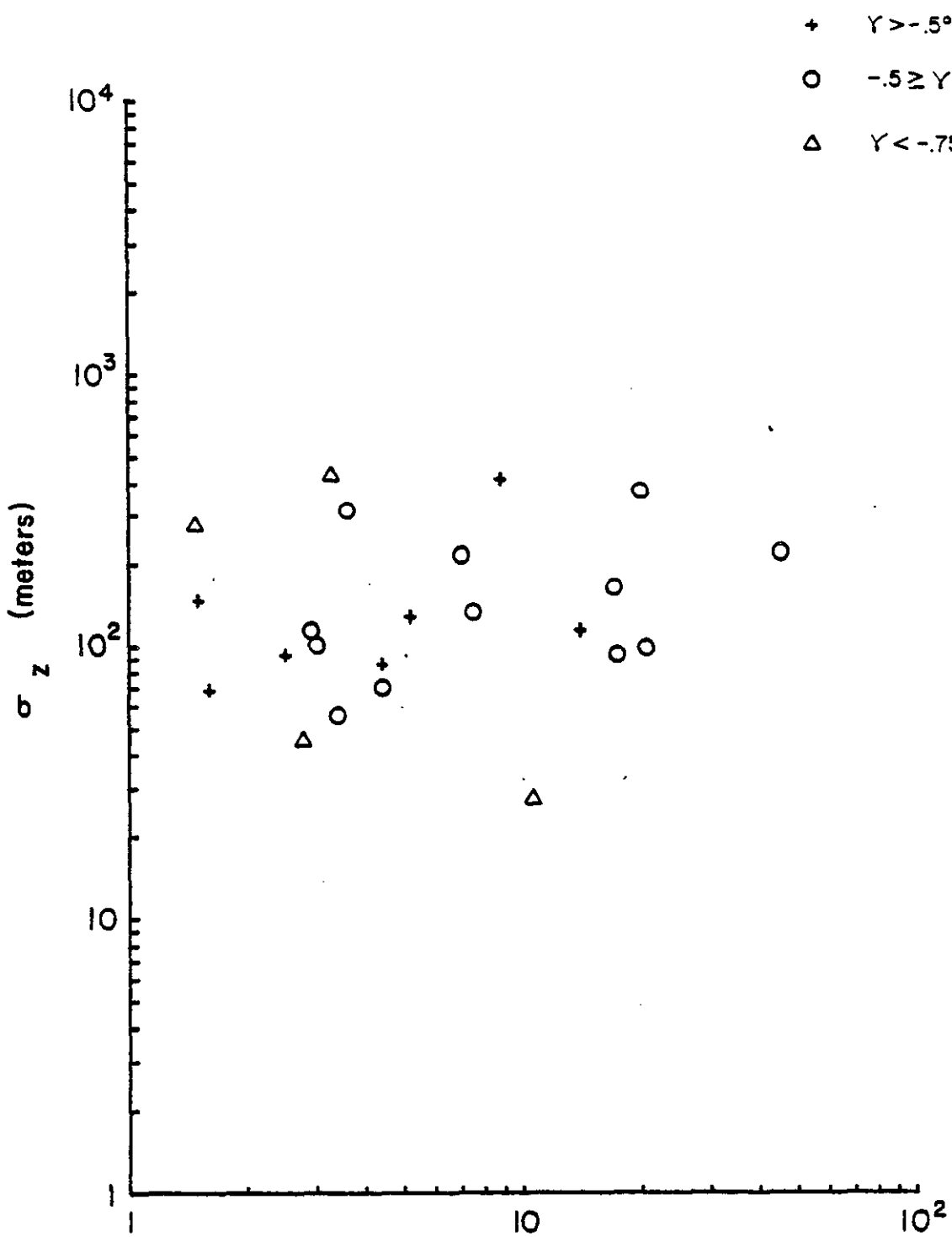

Figure (C)-5 σ_z Classified by Lapse Rate

804322

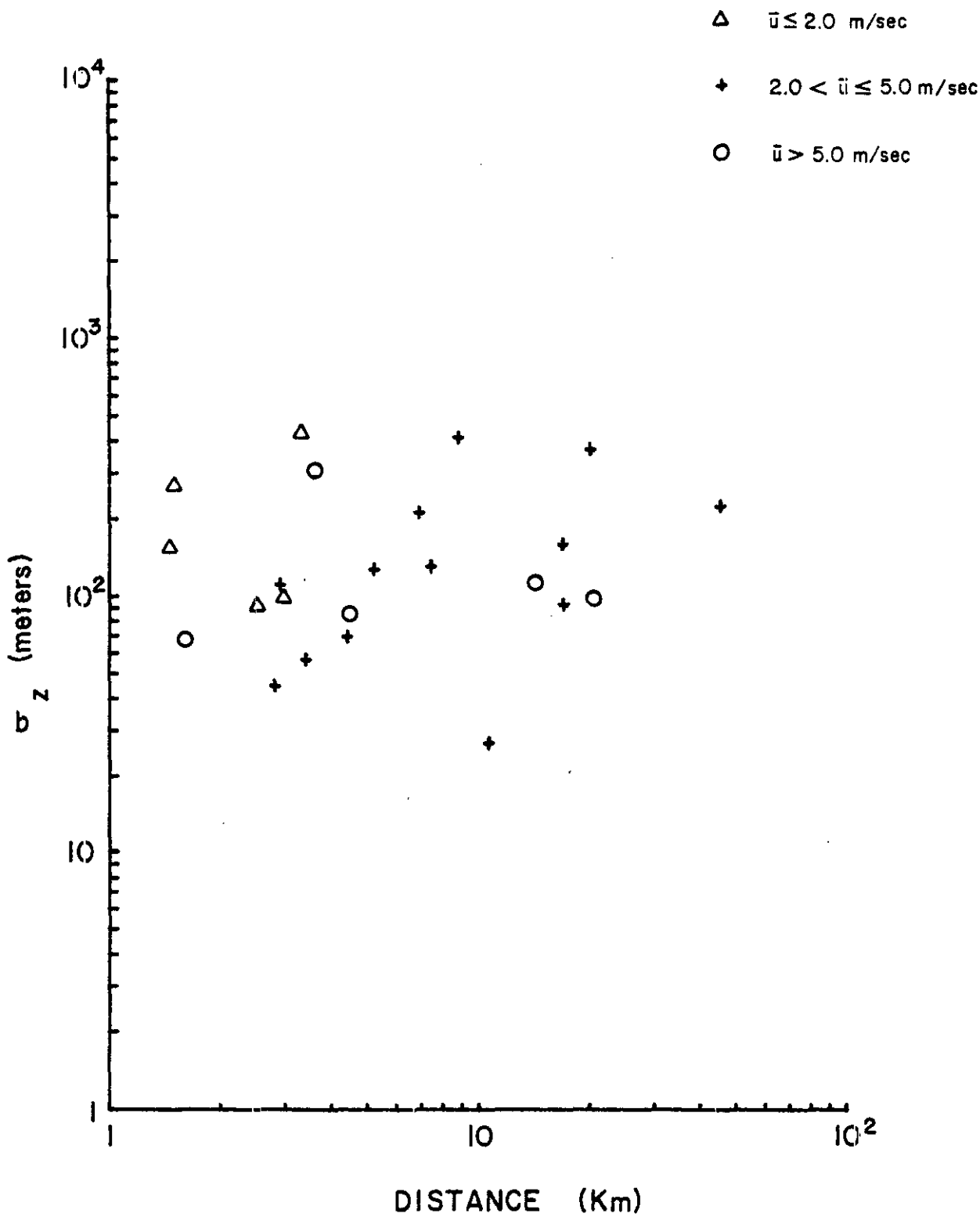

Figure (C)-6 σ_z Classified by Wind Speed

804323

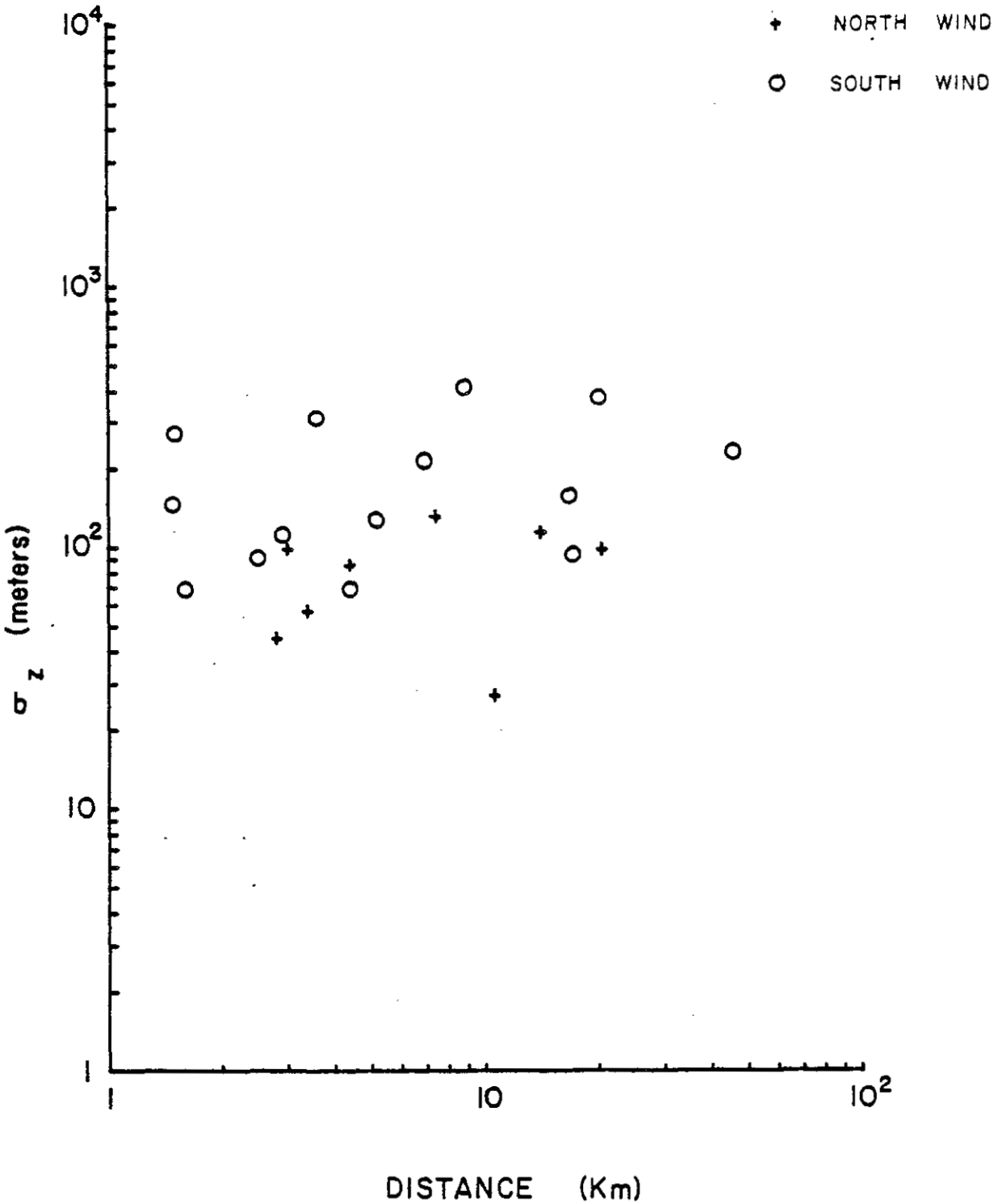

Figure (C)-7 σ_z Classified by Wind Direction

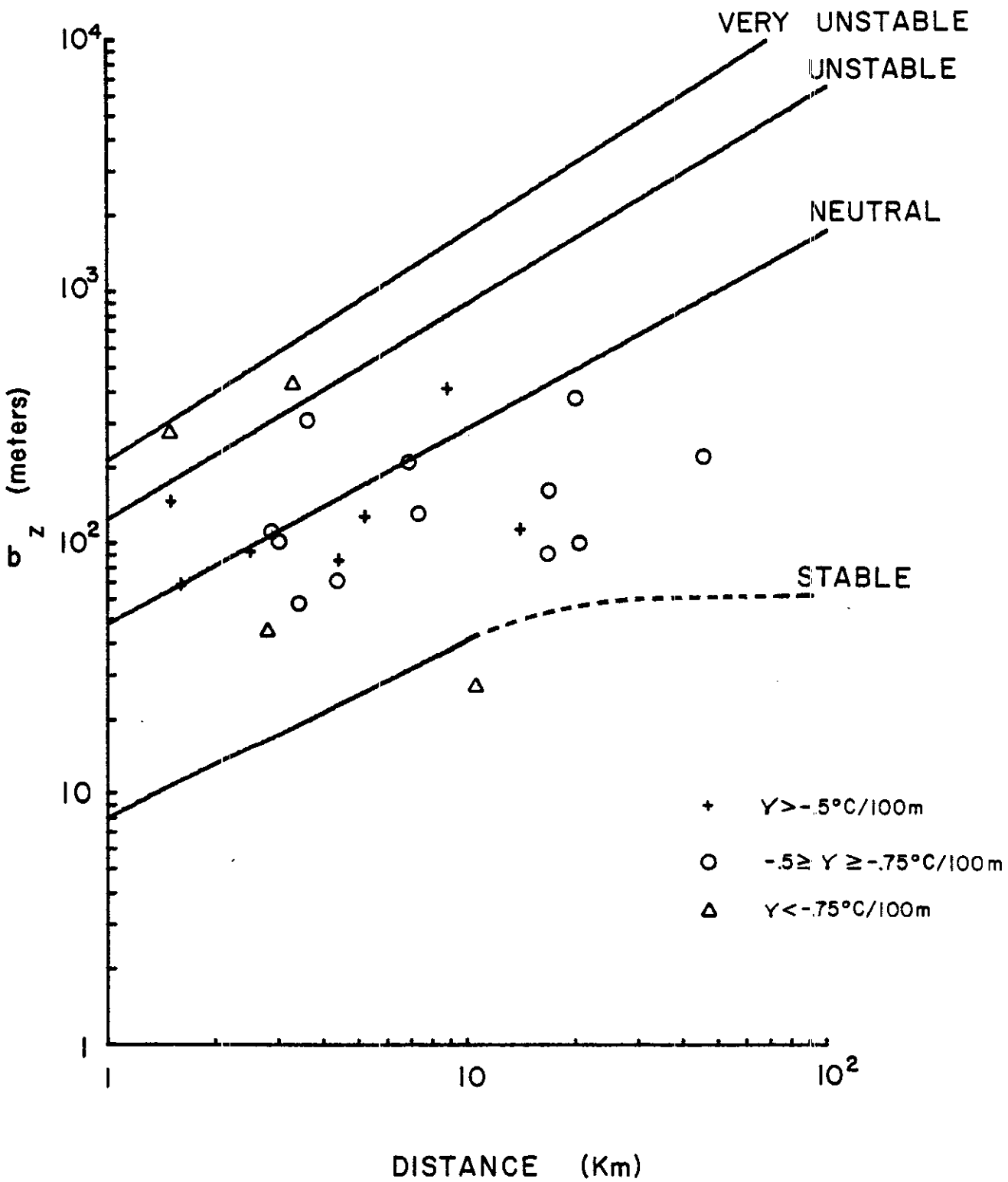

804326

Figure (C)-8 ASME Curves through σ_z Data

It is interesting that there is not a strong relationship between the plume spread statistics and wind direction (Figure (C)-3) considering that a slight difference in wind direction would transport the plume over vastly different terrain, which could induce large variations in σ_y. Due to difficulty in determining the exact location* of the plume and, subsequently, the nature of the terrain under the plume, or the height of the plume above the terrain during the tracer studies, a sound understanding of the effect of wind direction on plume spread cannot be obtained from the available data.

An examination of Figure (C)-4, which shows the measured Hat Creek σ_y's and the ASME curves, indicates that the curves are reliable parameterizations for predicting horizontal diffusion during atmospheric conditions which prevailed during the tracer studies. A statistical analysis, using the Student t-distribution, was performed to determine the error in σ_y based on the scatter of derived values for the 2 m/sec-5 m/sec wind speed class around the ASME neutral curve. It was found that the error in σ_y is $\pm$ 30%.

The errors shown in Table (C)-2 are due to errors in sampling and errors in the assumption of a Gaussian distribution. The average error shown in Table (C)-2 is $\pm$ 34%. Therefore, the total estimated error in the σ_y parameterization is about $\pm$ 45%.

(C)1.5 ANALYSIS OF σ_z

A graph of σ_z values categorized by lapse rate is provided in Figure (C)-5. Looping plumes were observed for two of the three tests during which the average lapse rate was less than -0.75°C/100 m. The wide scatter in the data is attributed to sampling problems under looping conditions. Statistical analysis shows that a random distribution of diffusion coefficients would have provided a better $\sigma_z = cx^d$ fit than the measurements 40% of the time. As Table (C)-3 indicates, σ_z has the highest correlation with lapse rate as compared with wind speed or wind direction.

*The NAWC plume location measurements were accurate within 0.5 km.

Figures (C)-6 and (C)-7 show σ_z categorized by wind speed and wind direction direction, respectively. It appears that south winds are generally associated with larger vertical diffusion than north winds. However, comparison with Figures (C)-5 and (C)-6 reveals that this trend may be associated with stability conditions and wind speed. In fact, the statistics cited in Table (C)-3 indicate there is a poor correlation of the σ_z values with wind direction and that the σ_z values are best correlated with lapse rate.

Results of NAWC tests 9 and 13 indicate substantial vertical plume growth under low wind speed (< 2.0 m/sec), plume looping (indicative of an unstable atmosphere) conditions. The resulting σ_z's are approximated by the 'very unstable' ASME curve (Figure (C)-8) for these tests. This approximation is valid because the unstable atmospheric conditions observed at Hat Creek are probably similar to those measured at the Brookhaven National Laboratory where the ASME curves were derived. NAWC reported strong looping conditions with little horizontal diffusion during these tests.

The graph of σ_z values derived from the Hat Creek tracer studies (Figure (C)-8) shows that the observed vertical temperature gradients, which are indicative of neutral or slightly stable atmospheric conditions, result in vertical plume dimensions that are close to those predicted by the 'neutral' ASME curve. The ASME parameterization scheme has, therefore, been selected to simulate the dimensions of the plume from the proposed Hat Creek Plant. An error analysis of the scatter of σ_z measurements around the ASME neutral curve was conducted and it was found that derived σ_z values approximate the ASME values within 30%.

(C)1.6 SELECTION OF A DISPERSION PARAMETERIZATION SCHEME

The analysis of the derived values of σ_y and σ_z showed that σ_y was well correlated with wind speed and that σ_z was correlated with lapse rate although two instances of looping plumes were observed with a neutral lapse rate* For light winds, values of σ_y taken from the ASME, very unstable and

*A lapse rate measured at plume height is usually a poor indicator of atmospheric turbulence. In general, atmospheric processes act to neutralize the state of the atmosphere and a superadiabatic lapse rate can be maintained only near the ground.

unstable curves appeared to best approximate the derived parameters. For moderate winds the neutral curve appeared to represent the derived values. Similarly, except for the looping plume cases, which were represented by the unstable ASME curves, the ASME neutral curve best represented the calculated σ_z's. To expand the model calibration to a wide variety of wind speeds and atmospheric stability conditions, the sigma-curves developed by Pasquill and Gifford, TVA, and ASME were considered according to the following criteria:

- the scheme must account for entire range of atmospheric stability conditions;
- the scheme must have been derived from tests or observations conducted at the same experimental location;
- the scheme must be applicable to elevated point sources; and
- the scheme must be consistent with the results of the Hat Creek tracer study.

It was found that the ASME parameters best represented the calculated values of σ_y and σ_z. Although standard sigma-curves are usually classified by atmospheric stability, the diffusion parameters will be used in the HCM according to both wind speed and stability classes (see Section (C)1.8).

The derived diffusion parameters were based on aircraft sampling times of 2 to 3 minutes. Although they will be used to calculate hourly average ground-level concentrations, no modifications to the magnitude of these parameters were made. In the atmosphere, plume dimensions relative to a fixed location increase as the averaging time increases because of the contribution of low frequency turbulence. On the other hand, turbulence rates and plume growth generally decreases with altitude. Because the trace experiments were conducted at elevations below those anticipated for the Hat Creek plume, ERT decided that the increase in plume growth with sampling time was compensated by the reduced growth with altitude so the derived diffusion and the selected ASME parameters were not modified.

(C)1.7 COMPARISON OF MODEL PREDICTIONS WITH GROUND MEASUREMENTS

There were four tracer tests during which ground level SF_6 concentrations were measured in sufficient quantities to obtain data for verification of the model calibration. These tests are numbers 2, 9, 12, and 13. Tests 2 and 9 are from tracer releases at the lower plant site and tests 12 and 13 are from the upper plant site.

A comparison of measured concentrations to computed concentrations using the HCM is provided in Table (C)-4. Because the exact location of the plume relative to the measuring device is difficult to determine from the data, several computations off the y-centerline are provided. It appears that the model substantially over predicts concentrations simulated for a plume release at the lower plant site, but does well for upper plant site emissions.

Caution should be observed in interpreting the results provided in Table (C)-4. There are many sources of error implicit in the analysis:

- the downwind distance is known to only $\pm$ 0.5 km;
- the location of the plume centerline relative to the ground sampler is highly approximate; and
- the calibration results show that vertical diffusion may be in error by $\pm$ 30% and horizontal diffusion by $\pm$ 45%; this corresponds to a predicted concentration inaccuracy of +112% to -51% or roughly a factor of two.

Because of these sources for error, it is difficult to comment on the reliability of the model from ground tracer data alone. Therefore, the HCM calculations of hourly ground-level concentrations are assumed to be accurate to within a factor of two based on the diffusion parameterization. The model calculations of concentrations for 3-hour and 24-hour averaging times are also considered accurate within a factor of two.

TABLE (C)-4

HCM COMPARISONS WITH SF_6 DATA

Test	Sampler	Distance (km)	Calculated SO_2 ($\mu g/m^3$)	Observed SO_2 ($\mu g/m^3$)	$\frac{SO_2 \text{ (Calc)}}{SO_2 \text{ (obs)}}$	Horizontal Distance from Plume Center (m)
2	2S4	4.8	1450	123	11.8	0
			960		7.8	250
			281		2.3	500
			2		0.02	1000
2	2S1	10.8	1140	73	15.6	0
			995		13.6	250
			660		9.0	500
			130		1.8	1000
9	4S1	3.8	6790	682	10.0	0
			6070		8.9	250
			4333		6.4	500
			1120		1.6	1000
9	4S4	4.4	6900	666	10.4	0
			6290		9.4	250
			4780		7.2	500
			1580		2.4	1000
9	4S2	5.0	3690	164	22.5	0
			3420		20.9	250
			2720		16.6	500
			1090		6.7	1000
9	4S6	2.4	918	1180	0.8	0
			749		0.6	250
			407		0.3	500
			36		0.03	1000

TABLE (C)-4
(Continued)

HCM COMPARISONS WITH SF_6 DATA

Test	Sampler	Distance (km)	Calculated SO_2 ($\mu g/m^3$)	Observed SO_2 ($\mu g/m^3$)	$\frac{SO_2 \text{ (calc)}}{SO_2 \text{ (obs)}}$	Horizontal Distance from Plume Center (m)
12	7S2A	9.7	580	866	0.7	0
			564		0.7	250
			518		0.6	500
			369		0.4	1000
12	7S3A	11.4	2060	1014	2.0	0
			2020		2.0	250
			1890		1.9	500
			1450		1.4	1000
12	7S9	14.4	871	1014	0.9	0
			858		0.8	250
			820		0.8	500
			684		0.7	1000
13	8S5	5.6	1410	162	8.7	0
			1320		8.2	250
			1080		6.7	500
			498		3.1	1000
13	8S6	3.5	276	300	0.9	0
			244		0.8	250
			167		0.6	500
			37		0.1	1000

(C)1.8 CONCLUSIONS

The results of the σ_y - σ_z analysis show that it is reasonable to categorize the horizontal and vertical plume dispersion using the split-sigma approach, i.e., that σ_y be categorized based upon the wind speed and σ_z be classified according to lapse rate.

A wider range of atmospheric conditions are expected to occur during the operation of the plant than those observed during the tracer studies. Therefore, results of the model calibration have been expanded to simulate a wider range of atmospheric conditions by application of the ASME parameters. Because the ASME curves provide a characterization of both σ_y and σ_z for the conditions of the NAWC tests and comply with the selection criteria in Section (C)1.6, the ASME curves are employed in the model to predict atmospheric diffusion under a wider spectrum of stability and wind speed conditions.

The following criteria are used in applying the ASME diffusion coefficients to the HCM.

Horizontal Dispersion Parameters

- Use the ASME very unstable curves for unstable conditions and wind speeds less than 2.0 m/sec.
- Use the ASME unstable curves for unstable conditions and wind speeds greater than 2.0 m/sec.
- Use the ASME unstable curves for stable and neutral conditions and wind speeds less than 2.0 m/sec.
- Use the ASME neutral curves for neutral and stable conditions and wind speeds greater than 2.0 m/sec.

Vertical Dispersion Parameters

- Use the ASME very unstable curves for unstable conditions and wind speeds less than 2.0 m/sec.
- Use the ASME unstable curves for unstable conditions and wind speeds greater than 2.0 m/sec.

- Use the ASME neutral curve when neutral and stable conditions prevail, regardless of the wind speed.

A summary of the dispersion coefficients and the meteorological criteria were presented in Table B4-1 in the main text of this Appendix and are summarized in Table (C)-5.

TABLE (C)-5

DISPERSION COEFFICIENTS DEVELOPED FOR THE HAT CREEK MODEL

Lapse Rate (γ) Category $^{o}C/100$ m	Wind Speed* (WS) Category (meters/sec)	Horizontal Dispersion Coefficients a	b
γ less than -1.5 (unstable)	WS less than 2.0	0.40	0.91
γ greater than -1.5 (neutral, stable)	WS less than 2.0	0.36	0.86
γ less than -1.5 (unstable)	WS greater than 2.0	0.36	0.86
γ greater than -1.5 (neutral, stable)	WS greater than 2.0	0.32	0.78

Lapse Rate (γ) Category	Wind Speed (WS) Category	Vertical Dispersion Coefficients c	d
γ less than -1.5 (unstable)	WS less than 2.0	0.40	0.91
γ less than -1.5 (unstable)	WS greater than 2.0	0.33	0.86
γ greater than -1.5 (neutral, stable)	any	0.22	0.78

*Wind speed measured at plume height.

(C)2.0 REFERENCES

1. Sagendorf, J. F. and C. R. Dickson 1974. Diffusion Under Low Windspeed, Inversion Conditions. NOAA Technical Memorandum. ERL ARL-52. Idaho Falls, Idaho.

2. Yanskeg, G. R., E. H. Markee, Jr. and A. P. Richter 1966. Climatology of the National Reactor Testing Station. IDO-12048. U.S. Atomic Energy Commission. Idaho Falls, Idaho.